JPL PUBLICATION 84-98

Final Report: Cosmic Ray Environment Model for Earth Orbit

L. Edmonds

January 15, 1985

NASA
National Aeronautics and Space Administration

Jet Propulsion Laboratory
California Institute of Technology
Pasadena, California

JPL PUBLICATION 84-98

Final Report: Cosmic Ray Environment Model for Earth Orbit

L. Edmonds

January 15, 1985

National Aeronautics and
Space Administration

Jet Propulsion Laboratory
California Institute of Technology
Pasadena, California

The research described in this publication was carried out by the Jet Propulsion Laboratory, California Institute of Technology, under a contract with the National Aeronautics and Space Administration.

ACKNOWLEDGEMENTS

I would like to give special thanks to Dr. Paul A. Robinson, Jr. of the Jet Propulsion Laboratory for providing some of the data and for providing advice throughout all stages of this study.

FOREWORD

By citing NPO-16617, Appendices C through G are available from COSMIC (Computer Software Management and Information Center), Suite 112, Barrow Hall, The University of Georgia, Athens, Georgia 30602.

ABSTRACT

This report describes a set of computer codes, which include the effects of the Earth's magnetic field, used to predict the cosmic ray environment (atomic numbers 1 through 28) for a spacecraft in a near-Earth orbit. A simple transport analysis is used to approximate the environment at the center of a spherical shield of arbitrary thickness. The final output is in a form (a Heinrich Curve) which has immediate applications for single event upset rate predictions. The codes will calculate the time average environment for an arbitrary number (fractional or whole) of circular orbit.

The computer codes are "stand alone" in the sense that they can be used individually for special applications, providing the necessary input data is given in the appropriate format. The codes are short enough to run on a desk top computer. The computer codes have been run for some selected orbits and the results, which can be useful for quick estimates of single event upset rates, are given. The codes have been listed in the language HPL, which is appropriate for a Hewlett Packard 9825B desk top computer. Extensive documentation of the codes is available from COSMIC, except where explanations have been deferred to references where extensive documentation can be found.

Some qualitative aspects of the effects of mass and magnetic shielding are also discussed.

CONTENTS

Figures

CONTENTS (Continued)

Figures

INTRODUCTION

In the last few years there have been a number of instances where a single cosmic ray particle has caused a device upset on space missions. This can occur when a single particle deposits enough charge in the sensitive region of a flip-flop circuit to cause a change of the state of the device. In many cases no permanent damage is done to the part, only the bit state is changed, hence the name "single event upset" (SEU). The current study is motivated by the need to calculate the likely upset rate for space systems due to high energy particles. This effort to understand and quantify single event upset phenomena has been used in predicting the upset rates of the Galileo project at JPL and has also been important in supporting other NASA and non-NASA projects.

Experiments on various Integrated Circuits (IC's) have shown that the most important parameter in determining the upset rate of the IC is the amount of deposited energy in a sensitive region in the part. This is most easily described in terms of the linear energy transfer (LET) of the particle as a function of energy. The linear energy transfer is the amount of energy lost by the particle as it passes through matter, or dE/dx. In its simplest form the probability of a particle causing an upset is found experimentally to be a threshold phenomenon when viewed as a function of the LET. For this reason it is useful to describe the environment in terms of particles with a specified LET or greater. Any particle with the minumum LET or greater will cause an upset with a constant (for this discussion) cross section. So in the programs developed for this study we compute what is called a Heinrich Curve, named after the man who first used it to describe the ability of cosmic rays to disrupt biological samples. The Heinrich Curve describes the flux of particles with a given LET or greater. This curve is used to estimate the SEU rate for parts.

The mass around a part will modify the number and LET of particles actually reaching the part so that the calculations need to include the effects of the mass. In general a three-dimensional calculation is needed to accurately describe this phenomenon. However, it is useful to estimate this effect by considering a part at the center of spherical shells of mass. Later, detailed calculations can be performed to determine the effects of the actual shielding provided.

The magnetic field around a planet or in a laboratory will also affect the particle flux. The effect of a magnetic field is to change the trajectory of the particle, but not its energy. For cosmic rays, the magnetic fields of the sun and the planets deflect the rays so that some do not reach volumes of space protected by the magnetic fields. This "shielding" removes lower energies from the spectrum and distorts the directionality of higher energy particles. Fortunately, all particles are affected in the same way in terms of a parameter called their rigidity. The rigidity of a particle is the momentum of the particle divided by the charge of the particle. Thus, for a given magnetic field and direction, only particles with a certain rigidity or greater can penetrate to that location.

This report describes a sequence of computer programs that will, when used together in sequence, produce a Heinrich Curve for cosmic rays (atomic numbers 1 through 28) for an arbitrary segment of a circular near-Earth orbit.

The sequence consists of five short programs which can be run on a desk top computer. The programs are all "stand alone" so they can either be run in succession to produce a Heinrich Curve for a near-Earth orbit or can be used individually for special jobs, providing the necessary input data is available in the appropriate format. For example, the first three programs will produce differential or integral spectra experienced by the exterior of the spacecraft and, together with the fourth program, they will produce integral spectra inside a spherical shielded region. If a spectrum is provided by other methods (for example a spectrum that includes trapped particles and cosmic ray particles near Jupiter), the spectrum can be loaded in a data file and the last three programs can be used to obtain the Heinrich Curve for that environment.

The programs are as follows:

GEOMAG*:	Calculates a modulating factor due to geomagnetic shielding for a given trajectory segment which, when multiplied by the interplanetary spectrum, produces the time averaged spectrum experienced by the spacecraft. This program, and only this program, requires information about the trajectory segment.
SPECTRUM**:	Calculates the interplanetary cosmic ray spectra at 1 AU and multiplies them by the modulating factor calculated by GEOMAG to produce a time average of the spectra seen at the exterior of the spacecraft.
INTEGRATE:	A short, simple integration to convert differential spectra to integral spectra.
TRANSPORT:	Takes the output of the program INTEGRATE and calculates the integral flux at the center of a spherical shielded region.
UPSET FLUX:	For each of a discrete set of values of the threshold LET, this program takes the output of TRANSPORT and calculates the flux of particles that will cause upsets.

Program GEOMAG obtains a modulating factor for a segment of a circular orbit which accounts for the shielding of the Earth's magnetic field. The segment can be of any size and it can be an isolated point. To get a time

*This program was originally written in a longer version by J. H. Adams, Jr., J. R. Letaw, and D. F. Smart, and can be found in reference (1).
**This program uses the algorithms provided by J. H. Adams, Jr., R. Silberberg, and C. H. Tsao in reference (2).

average spectrum for a long complex flight pattern, an auxiliary driver program that drives GEOMAG can be constructed which has the flight path built into it. The driver would direct GEOMAG to evaluate the modulating factor at various points and the driver would calculate the time weighted average of the results. Without this auxiliary driver GEOMAG will obtain the modulating factor for an arbitrary number (fractional or whole) of circular orbits. In particular we can use isolated points*, and a succession of runs can be done manually to produce a history of the flux. This history would be in the form of a sequence of Heinrich Curves representing a sequence of discrete points on an arbitrary flight path.

Chapter 1 of this report describes the theory and calculational algorithms used by programs GEOMAG, SPECTRUM, TRANSPORT, and UPSET FLUX. A computer printout of the actual programs, written for a Hewlett Packard 9825B desk top computer, combined with brief explanations of the program lines, are included in Appendices C through G.** The language used is HPL. The programs were printed out on the HP 82905B printer. It should be noted that "}" represents "→" and "{" represents "π" and "\" represents "√ ".

Chapter 2 discusses the qualitative aspects of the effects that the combination of mass shielding and geomagnetic shielding have on the Heinrich Curves. These qualitative discussions are supported by the numerical results found in Appendix A which contains the results of actual computer runs made for a number of specific cases. The reader may find Appendix A to be useful for quick estimates of the upset rates that may occur for a part having given characteristics and in a given near-Earth orbit.

Chapter 3 discusses limitations and sources of error in the assumptions used in the various programs.

*Limitations on the validity of the results for isolated points are discussed in Chapter 3.

**Appendices C through G can be obtained by writing to: COSMIC, Suite 112, Barrow Hall, The University of Georgia, Athens, Georgia 30602.

CHAPTER 1

THEORY AND METHODS OF THE COMPUTER PROGRAMS

THEORY AND METHOD OF GEOMAG

The theory behind GEOMAG is given in reference (1) and will only be briefly outlined here. GEOMAG consists of a subroutine called STORMER and a sequence of steps that prepares data for STORMER and calls STORMER. This sequence of steps will be called the driver program. The driver program given in this report is similar to the version given in reference (1). One difference between the two versions is that the driver given in this report accepts an arbitrary number of time steps; whereas, the original version samples an orbit over a two-day period. Another difference is that the version given here does not include the compression of the Earth's magnetic field due to major solar flares. The only other difference is that this version provides the option of printing the cutoff rigidity at each time step, not printing it at any time step, or printing extreme values (relative minimums and maximums).

The basic theory is as follows. If we measure the differential directional intensity at a given location in a localized static magnetic field, looking in a given direction, we can find a "rigidity" (momentum divided by charge of an incoming particle) called the STORMER CUTOFF. The STORMER CUTOFF has the property that no particle originating from outside the magnetic field with rigidity below this cutoff can reach the given location from the specified direction. If a particle with rigidity below this cutoff is found at this location traveling in this direction, it is a trapped particle. The particle could not have arrived from infinity and cannot escape to infinity without a change in charge state (which changes its rigidity) or interference by other forces. In general, the STORMER CUTOFF is a function of both the point of observation and the direction of observation. The differential directional intensity at a given location looking in a given direction is zero (if the measurement does not record trapped particles) at all energies below the value corresponding to the STORMER CUTOFF rigidity for that location and direction.

There is also another kind of cutoff rigidity, called the MAIN CONE CUTOFF, also a function of position and arrival direction, with the property that any particle with rigidity greater than the MAIN CONE CUTOFF did come from infinity (or an effectively infinite distance, i.e., from interplanetary space). It follows from Liouville's theorem that a measurement of the differential directional intensity at a given location in a given direction will produce the interplanetary value at all energies above the energy corresponding to the MAIN CONE CUTOFF. From the previous discussion this same measurement will produce zero (it will be assumed from this point on that trapped particles are excluded from consideration) at all energies below the energy corresponding to the STORMER CUTOFF. It is difficult to compute fluxes at rigidities between the STORMER CUTOFF and MAIN CONE CUTOFF. Fortunately, this interval is often sufficiently narrow that the concept of an "EFFECTIVE CUTOFF" becomes useful. This EFFECTIVE CUTOFF, which is between the STORMER and MAIN CONE CUTOFFs,

provides us with an approximation if we assume it has the properties that: 1) all rigidities below this cutoff are associated with a zero differential directional intensity; and 2) all rigidities above this cutoff are associated with the interplanetary space value of the differential directional intensity. This EFFECTIVE CUTOFF is discussed in reference (3).

In addition to the use of an EFFECTIVE CUTOFF we also use another approximation, which is to regard the flux at a given observation point as though it were isotropic with a value in a given direction being equal to what is predicted by using the "vertical cutoff" (the EFFECTIVE CUTOFF evaluated perpendicular to the Earth's surface). So although a directional dependence exists for the cutoff, this directional dependence is removed from consideration in our treatment of the problem. Limitations of this approximation are discussed in Chapter 3.

The driver portion of GEOMAG calculates the spacecraft location for each of a discrete set of values of time. A table of EFFECTIVE CUTOFF rigidities for a 20-km altitude at various latitudes and longitudes forming a grid are given in reference (3) and are loaded in the program.* At the four grid points surrounding the spacecraft latitude and longitude, the theoretically predicted STORMER CUTOFFs are calculated by calling the subroutine STORMER. These cutoffs are calculated from the equation appropriate for a magnetic dipole which is oriented and located to best fit the Earth's magnetic field, and the cutoffs are calculated for the locations of the grid points. At each of the four grid points, the ratios of the tabulated EFFECTIVE CUTOFFs to the calculated STORMER CUTOFFs are formed. These ratios are interpolated to the spacecraft latitude and longitude. Finally, the interpolated ratio is multiplied by the theoretically predicted STORMER CUTOFF evaluated at the spacecraft location. These steps produce a combination of interpolation and extrapolation of the EFFECTIVE CUTOFF and the result is an approximation of the EFFECTIVE CUTOFF at the spacecraft location. These steps are repeated for each of a discrete set of values of time, i.e., for each "time step," and a counting scheme is used to enable the program to produce a time average of the transmission function, which is the output of the program. This transmission function has the property that when multiplied by the differential interplanetary spectrum, the result is the time average differential spectrum experienced by the spacecraft.

The subroutine STORMER has been drastically shortened from the original version found in reference (1). It was determined that the original version is much more elaborate than is needed. The two versions produce values for the transmission function that agree to three significant digits ("transmission function" is the name given to the modulating factor described in the introduction). Many of the tabulated values show exact agreement, but this is because the transmission function can only take on discrete values due to the nature of the programs (it is calculated by counting elements in "bins"). A brief discussion of STORMER is given below.

*A listing of these data is also given in reference (1) but this listing contains misprints. A corrected listing is given in Appendix C.

The Earth's magnetic field is approximated by an offset dipole. The dipole moment used in STORMER is treated as independent of time and has the following characteristics (taken from reference (4)). It is located at a distance of 436 km from the center of the Earth towards a point at 15.6° N latitude and 150.9° E at 81° N latitude, 84.7° W longitude and at 75° S latitude, 120.4° E longitude. This information together with elementary vector analysis will provide a transformation between the geocentric latitude, longitude, and altitude of a point and the latitude in dipole coordinates and distance from the dipole to the point. (By "dipole coordinates" we mean the coordinates in a coordinate system with origin at the dipole and the Z axis along the dipole moment.) The coefficients in this transformation are not calculated by STORMER. They were calculated once and are contained in STORMER.

To obtain the STORMER CUTOFF for a dipole, two things must be known: the dipole coordinates of the point in question and the arrival direction. When STORMER is called, a space point is given to STORMER and STORMER first calculates the dipole coordinates of that point. An arrival direction must also be specified. The arrival direction is taken to be perpendicular to the Earth's surface, which is the direction to which the tabulated values for the EFFECTIVE CUTOFF apply. This is not quite the same as being radially outward in dipole coordinates, but it was found that it is close enough for the difference to be negligible as far as the final output of STORMER is concerned. STORMER then takes the dipole coordinates of the space point and puts them into the equation for the STORMER CUTOFF for a dipole. This equation is in a simplified form because it applies to the special case of an arrival direction that is radially inwards in dipole coordinates. The general form of the equation is

$$\text{cutoff rigidity} = \frac{3 \times 10^{-14} \, M \cos^4 A}{r^2 \left(1 + \left(1 - \cos B \cos^3 A\right)^{1/2}\right)^2}$$

where the cutoff rigidity is in units of GeV/ec. M is the magnetic dipole moment in units of amp-meter^2 (for Earth, $M = 8.06 \times 10^{22}$), A is the magnetic latitude, B is the angle between the particle arrival direction and magnetic east, and r is the distance in kilometers from the dipole to the point of observation. For a radial arrival direction ($B = 90^\circ$) the equation reduces to

$$\text{vertical cutoff} = 7.5 \times 10^{-15} \frac{M \cos^4 A}{r^2}$$

The STORMER CUTOFF so computed is the final result returned by STORMER.

THEORY AND METHOD OF SPECTRUM

The calculational algorithms used in SPECTRUM to construct the interplanetary cosmic ray spectra were taken directly form reference (2). Because there is still much uncertainity in the "anomalous component" described in reference (2), it was not included. Fortunately it is not difficult to

provide protection against this component. Reference (2) states that the important contribution of the anomalous component is to the nitrogen and oxygen spectra (up to 30 MeV/nucleon) and to the helium spectrum (up to 200 MeV/nucleon). Depending on the orbit and ionization state of the anomalous component, these particles may or may not be blocked by the geomagnetic field, but the contribution to the oxygen and nitrogen spectra are easily blocked by mass shielding (1.3 mm of aluminum is sufficient). The higher energy helium ions are much more penetrating, but a radiation hard part (with a threshold LET above 2 MeV-cm^2/mg) will not see upsets from these ions by direct ionization. If the spacecraft does not have this protection, or if spallation reactions are significant, the anomalous components will have to be included as a separate consideration. Reference (2) contains information on this subject.

SPECTRUM first computes the spectra for hydrogen, helium, and iron. These spectra are then multiplied by the transmission function, which was computed by GEOMAG, and evaluated at the appropriate rigidity. The point of evaluation of the transmission function depends on the charge state. Hydrogen is assumed to be singly ionized. The charge state of all other species is assumed to be one half the atomic mass.

At high inclination orbits the transmission function differs from zero at very low energies, and the coarseness of the computed tabulation of the transmission function makes interpolation questionable. A worst case calculation is obtained by selecting independent values of energy to evaluate the interplanetary spectra and then computing the rigidity associated with this energy (with a charge state assumed). This rigidity is compared to the values in the tabulation of the transmission function. The value of the transmission function at the lowest tabulated rigidity that is greater than or equal to the calculated rigidity is used. This insures a worst case estimate because the transmission function is a monotonically increasing function of rigidity.

The spectra for all other species with atomic numbers up to and including 28 are obtained from the helium and iron spectra using the procedures given in reference (2). Since the transmission function has already been included in the helium and iron spectra, it is automatically included in all remaining species.

The output of SPECTRUM is a time-averaged (averaged over the time interval used by GEOMAG in calculating the transmission function) differential cosmic ray spectrum seen by the spacecraft for each species from atomic numbers 1 to 28. These data are stored in a set of data files, one data file for each atomic number.

THEORY AND METHOD OF TRANSPORT

After running program SPECTRUM, another program called INTEGRATE is used to convert the differential spectra produced by SPECTRUM into integral spectra. INTEGRATE is short and simple and uses a 201 point fit trapezoidal integration. A listing of the program is given in Appendix E. The output of INTEGRATE is a

set of data files, with each data file containing the integral spectrum for a single species. All species from atomic numbers 1 through 28 are included.

TRANSPORT uses these data to construct the integral spectrum for each species at the center of a spherical shielded region. It is assumed that the shield is of uniform thickness and that the flux exterior to the shield is isotropic. Spallation, straggling, and bremsstrahlung are not included.

Each species is treated separately. For a specific species, let E be an independently selected value of energy to be used as the point of evaluation of the integral flux at the center of the shielded region. Let E' be the energy satisfying the condition that a particle exterior to the shield with energy E' will, after traveling through the thickness of the shield, emerge with energy E. Note that since the shield is spherical with uniform thickness and the observation point is at the center, all particles reaching the observation point must (to the extent that straggling can be neglected) travel through the same path length, the thickness of the shield. The integral flux at the center evaluated at E will equal the integral flux exterior to the shield evaluated at E'.* So the problem reduces to the determination of E' when E is given.

Let R denote the range function and L denote the shield thickness. E and E' are then related by

$$L = R(E') - R(E)$$

or

$$E' = R^{-1}(L + R(E))$$

The previous equation is solved by TRANSPORT by interpolating a tabulation or R versus E. This tabulation is stored in a data file that is input to the program.

The tabulation of R versus E was obtained from information given in reference (5). Reference (5) contains a tabulation but unfortunately it only extends up to 12 MeV/nucleon which is not nearly high enough for this application. But dE/dX curves are also given and these curves range from very low energies to 10^5 MeV/nucleon (with a very small amount of extrapolation). A numerical integration using these curves will produce the desired range tables. Not all species are represented by the curves given in reference (5). The procedure was to perform the numerical integration to obtain range tables for species that are represented. The range tables were then used to obtain range tables for other species by interpolation. At a given energy per nucleon, the atomic number was used to interpolate between values of the range function. This interpolation is the procedure suggested in reference (5).

*See Appendix B for a derivation of this.

It is an important point that the numerical process just described was used to extend the range tables given in reference (5) beyond 12 MeV/nucleon. Below 12 MeV/nucleon, the range tables of reference (5) were used. The range tables of reference (5) were constructed using detailed calculations that made corrections for nuclear stopping power, so that the range tables are associated with a total stopping power rather than the electronic stopping power alone. The extension of the range tables was done over energies where there is no distinction between total and electronic stopping power, so the range data used by TRANSPORT are associated with the total stopping power.

The range data used by TRANSPORT are listed in Appendix F immediately after the program listing. The output of TRANSPORT is a set of data files. Each data file is an integral flux spectrum at the center of the shielded region, one data file for each species.

THEORY AND METHOD OF UPSET FLUX

UPSET FLUX takes the integral spectra computed by TRANSPORT and converts them into a Heinrich Curve described in the Introduction of this report.

Since single event upset rates are additive, Heinrich Curves for different particle species are additive. UPSET FLUX looks at one species at a time and for each species it computes the Heinrich Curve associated with that species and adds it to a running total.

The Heinrich Curve for a given species is computed according to the following reasoning. For a given species traveling through a given material, the linear energy transfer (LET) is a well-defined function of energy. The objective is to select a set of LET values and, for each value selected, determine the number of particles with LETs greater than this value, and tabulate these fluxes against the set of LET values selected. We obtain the flux of particles with LET greater than a given value by referring to the LET versus energy curve. If the LET value selected is not greater than the maximum LET of the particle (if it is we simply set the flux equal to zero), we can find one and sometimes two energy intervals such that at all energies in these intervals the LET is greater than the value selected. Integrating the differential flux over these energy intervals produces a total flux (number of particles per area per time) of the given species with a LET above the selected value. What is equivalent to integrating the differential flux over the selected energy intervals is to take sums and differences of the integral flux evaluated at the obvious energies. This is what UPSET FLUX does. Two sets of data are input to UPSET FLUX: a tabulation of integral flux (for each species) versus energy and a tabulation of the energy integration limits (for each species) versus LET. For a given LET, the energy integration limits are used as the points of evaluation of the integral fluxes to be added and subtracted to obtain a total flux of particles with LET greater than the given value. For each LET value there are four energy integration limits because of the possibility of two distinct energy intervals. When there is only one energy interval, two integration limits will be equal to each other.

The sets of integration limits versus LET were obtained from the stopping power curves of reference (5). It should be noted that the curves of reference (5) should be mutliplied by the square of the atomic number of the particles to obtain the LET, which is -dE/dX. It should also be noted that the electronic stopping power (rather than total stopping power) curves should be used because the Heinrich Curves are intended to predict rates of single event upsets due to direct ionization.

The table of integration limits used by UPSET FLUX is given in Appendix G immediately after the listing of the program. The output of UPSET FLUX is a data file which is a tabulation of the flux of particles with LETs above a threshold value versus threshold values.

CHAPTER 2

QUALITATIVE CHARACTERISTICS OF THE EFFECTS OF MASS SHIELDING AND GEOMAGNETIC SHIELDING

The observations to be discussed are not as pronounced in the actual case, where there is a mixture of cosmic ray particle species modulated by a complicated transmission function, as they would be if only one species were present and the tramsission function were a simple step function. Nevertheless a number of qualitative effects of mass shielding and geomagnetic shielding are still observable. To simplify the discussion of these considerations we will assume, until stated otherwise, that only one particle species is present and we will look at an isolated point in space so that the transmission function is a simple step function.

The magnetic cutoff removes particles with energy less than the cutoff. Mass shielding degrades the energy of all particles. This changes the distribution of particles behind the shield and in particular it repopulates the low energy portion of the spectrum.

A typical LET versus energy curve is sketched in Figure 2.1. At sufficiently low energies the LET is an increasing function of energy, at higher energies it is decreasing, and at very high energies it is increasing again. These different behaviors result in differenet qualitative effects of mass and magnetic shielding. For this reason it is convenient to group magnetic cutoffs into the categories of low, medium, and high. To be more precise, refer to Figure 2.1; low cutoff is below E1, medium is between E1 and E2, and high is above E2. The section of the curve above the intervals denoted as low cutoff and medium cutoff will be called the "bump." The section above the low cutoff interval and the section above the medium cutoff interval will be called the left side and right side of the bump, respectively. The region above the high cutoff interval will be called the "tail." At any given cutoff, we can also look at low and high values of the LET. We will say a LET is high or low depending on whether it is above or below L2 (shown in Figure 2.1). The trivial case of LET above L1 leads to zero upset flux regardless of magnetic or mass shielding. Depending on the cutoff, mass shielding can effect the low LET section of the Heinrich Curve differently than it effects the high section.

Regardless of the magnetic cutoff, the effects of mass shielding at the low LET section of the Heinrich Curve are governed by the same simple principle, although the conclusion based on this principle will depend on the cutoff. At low theshold LETs all particles that hit the part`s sensitive region will cause an upset regardless of the energy of the particle.* The effect of

*There are complications that we are neglecting. First, the total energy of the particle must be at least as high as the threshold energy of the part. Any errors resulting from neglecting this will be in the direction of a worst case prediction of upset rates. Second, the threshold LET depends on geometric factors in such a way that it isn`t correct to associate a single threshold LET with the part. Depending on the part, it may be justifiable to do this for order of magnitude estimates. See Chapter 3.

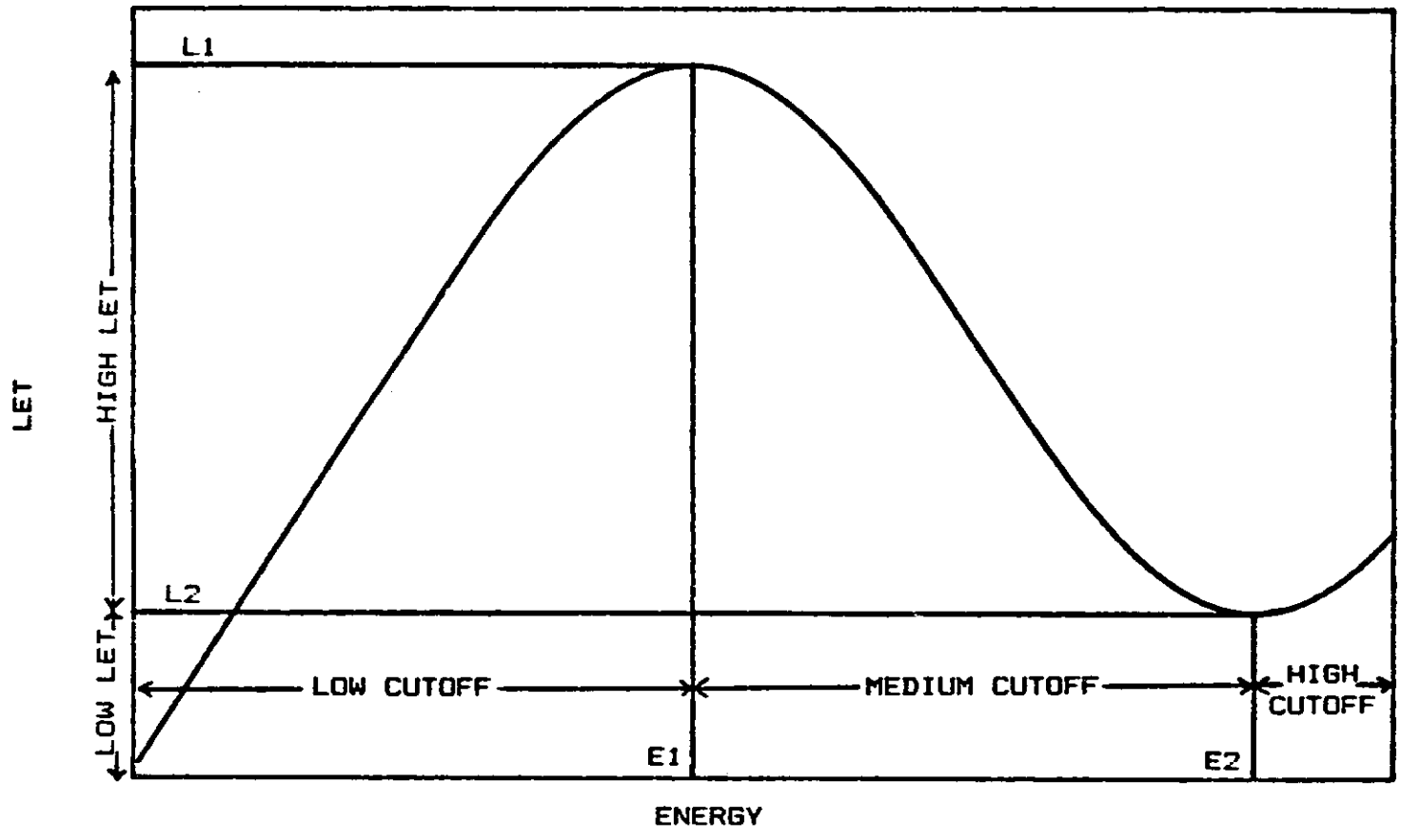

Figure 2.1. Sketch of typical log-log plot of LET vs. energy.
E2 is approximately 2 GeV/nucleon.
E1 is typically on the order of 1 MeV/nucleon.

mass shielding on the energy of the particle is irrelevant. All that matters is the number of particles blocked by the shield. At high cutoffs few if any particles are blocked (unless the shield is very thick) so we expect the shield to make little if any difference in the Heinrich Curve at low LETs. Even at very low cutoffs, the effect of mass shielding may be small (less than a factor of 2 in the upset flux for shielding thicknesses normally used in practice) depending on the spectrum used. SPECTRUM provides the option of using or not using a worst case, low energy spectrum which includes particles from small solar flares and particles accelerated in the interplanetary medium combined with a 90% confidence level. This is discussed in reference (2). At low cutoffs, but without this worst case, low energy spectrum, there are some particles that can be blocked by a moderate shield but not many compared to the total number of particles. It is not expected that a shield will make a great deal of difference at the low threshold LETs. If the worst case spectrum is used, a much larger fraction of particles are at energies low enough to be blocked by a moderate shield and the effect of mass shielding at the low LETs is much larger. This is demonstrated in Figures A.15 and A.16 of Appendix A. When the worst case spectrum is not used, the upset flux for a 100-mm aluminum shield differs from that for a 0.63-mm shield by less than a factor of 2 at the low LETs. Making this same comparison when the worst case spectrum is used shows a difference of about a factor of 27.

The effects of mass shielding at high LETs is more subtle. The different cases are discussed categorically below.

LOW MAGNETIC CUTOFF

As just discussed, at a low cutoff and low LET, we would expect mass shielding to make a small but observable difference in the Heinrich Curve if the worst case, low energy spectrum is not used. This is demonstrated in Figure F.15. We would expect the effect to be much greater if the worst case spectrum is used. This is demonstrated in Figure F.16.

Similar considerations also apply to the high LET case. Let us look at a typical low cutoff, which is denoted by EC in Figure 2.2, and a typical high LET value denoted by L in the figure. E`, E``, and E``` are determined by the intersection of the L line with the LET curve as shown in the figure. The energy values that would produce upsets if populated with particles are the ones between E` and E`` and the ones above E```. Without mass shielding, energy values with a non-zero particle population are above EC. So without mass shielding there are particles that will cause upsets occupying the left side and right side of the bump. If a shield is now put in place and the shield is not extremely thin, a large population of particles with energies under the bump will have their energies shifted to the left in Figure 2.2 across the E` line (many particles would be blocked by the shield which would be represented in Figure 2.2 as being shifted to zero or negative energies) where they can no longer contribute to upsets. This tends to deplete the region between E` and E`` of particles.

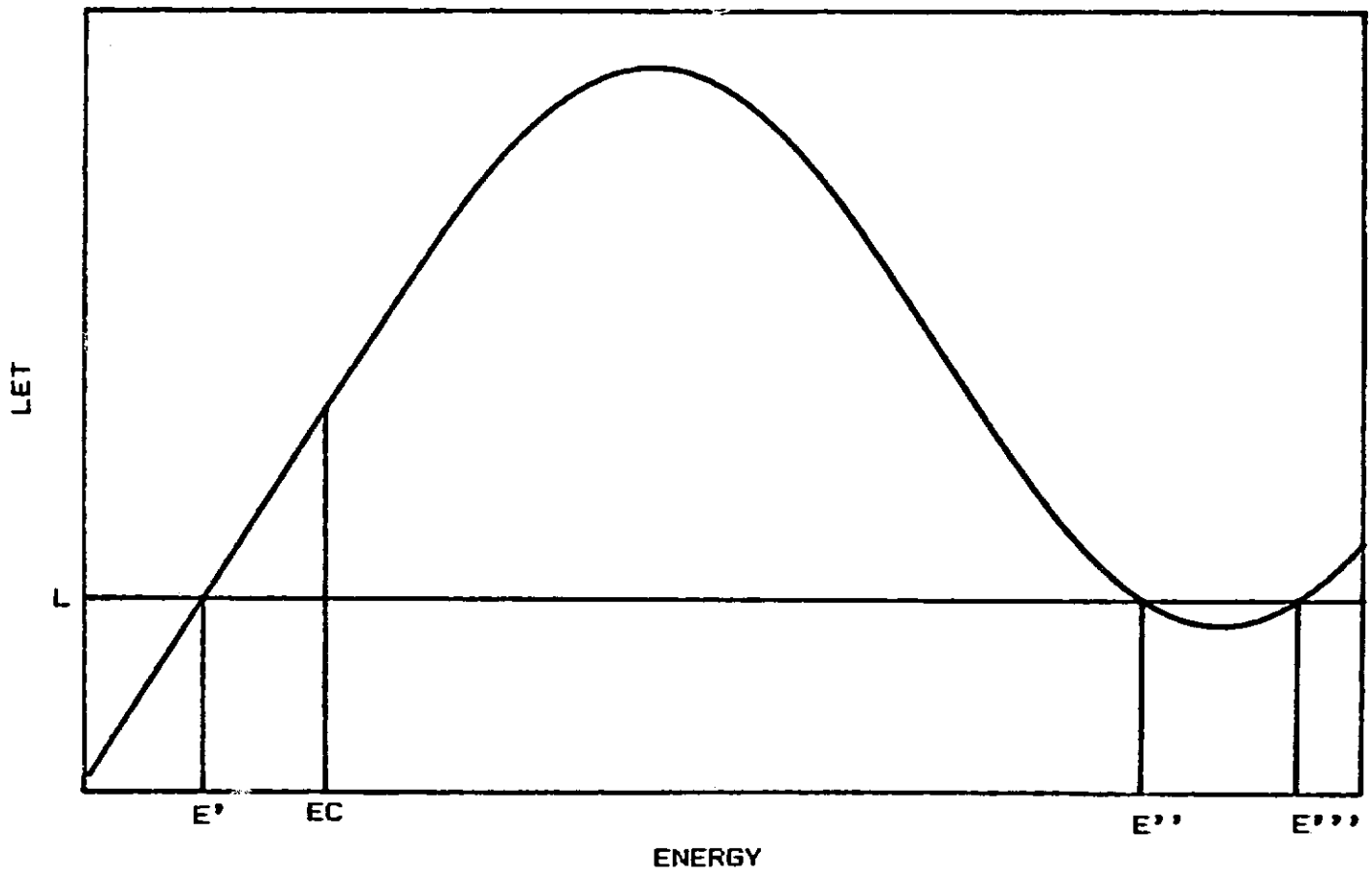

Figure 2.2. LET vs. energy curve showing typical low cutoff EC and typical high LET denoted by L.

It is true that there are also particles with energies initially (before the shield was put in place) above E`` so that they now cause upsets when they originally would not have. But these higher energy particles have lower LETs than the particles with energies below E`` (as is seen in figure 2.2). Also, their energies were significantly higher so there is a smaller fractional change in energy as they pass through the shield. This means their LET remains low as they pass through the shield. Therefore, they are not effected as much by the shield as the lower energy particles. The higher energy particles whose energies were brought below E`` came from a relatively narrow energy interval that is bounded on the left by E`` and, therefore, there are comparatively few of these particles (unless the differential spectrum is much larger at E`` than at the lower energies). We would expect the depletion of particles with energies between E` and E`` due to particles moving to the left of E` to more than make up for the enhancement of this population due to particles moving to the left of E``. The tendency of the net effect is to decrease the upset flux. There are also particles in the tail moving to the left of E``` due to the shield, but these very high energy particles are negligibly effected by the shield. So we expect the effects of mass shielding to be a decrease in upset flux at high LET values. A word of caution is in order here. To demonstrate the effect described we must compare the 0.63-mm shield to a heavier shield because SPECTRUM sets the differential flux to zero below 10 MeV/nucleon and a thin shield is required to populate the low energies. If we compare a shielded case to no shielding we will be seeing the properties of the medium cutoff case because of the termination of the spectrum below 10 MeV/nucleon. If we increase the shielding thickness from zero we will first see an increase in upsets at the high LETs as predicted by the medium cutoff case (to be discussed later). After so much shielding has been added the low energies are populated and we are simulating the low cutoff case so further increases in shield thickness will decrease the upset flux.

In summary, for low magnetic cutoffs we expect the effect of mass shielding to be a lowering of the Heinrich Curve at both low and high LET values. This is demonstrated in Figures A.15 and A.16.

MEDIUM MAGNETIC CUTOFF

As previously discussed, the effect of mass shielding on the Heinrich Curve at low LETs goes with the number of particles blocked by the shield. A medium magnetic cutoff can occur anywhere between ~1 MeV/nucleon and about 2 x 10^3 MeV/nucleon. So the effect of mass shielding at the low LETs may or may not be observable depending on just where the cutoff is. If the effect is observable, the effect will be to lower the Heinrich Curve.

To see the effect of mass shielding at high LETs, refer to Figure 2.3 which shows a typical medium cutoff denoted by EC and a special value of LET denoted by L. Let E` and E`` be as shown in the figure. We are looking at a special value of LET because, as will be seen, not all high LET values have the property this one has.

Energies under the bump that would cause upsets at this LET if they were populated with particles are between E` and EC. Before the shield is in place there is no population of particles in this region so there will be no upsets

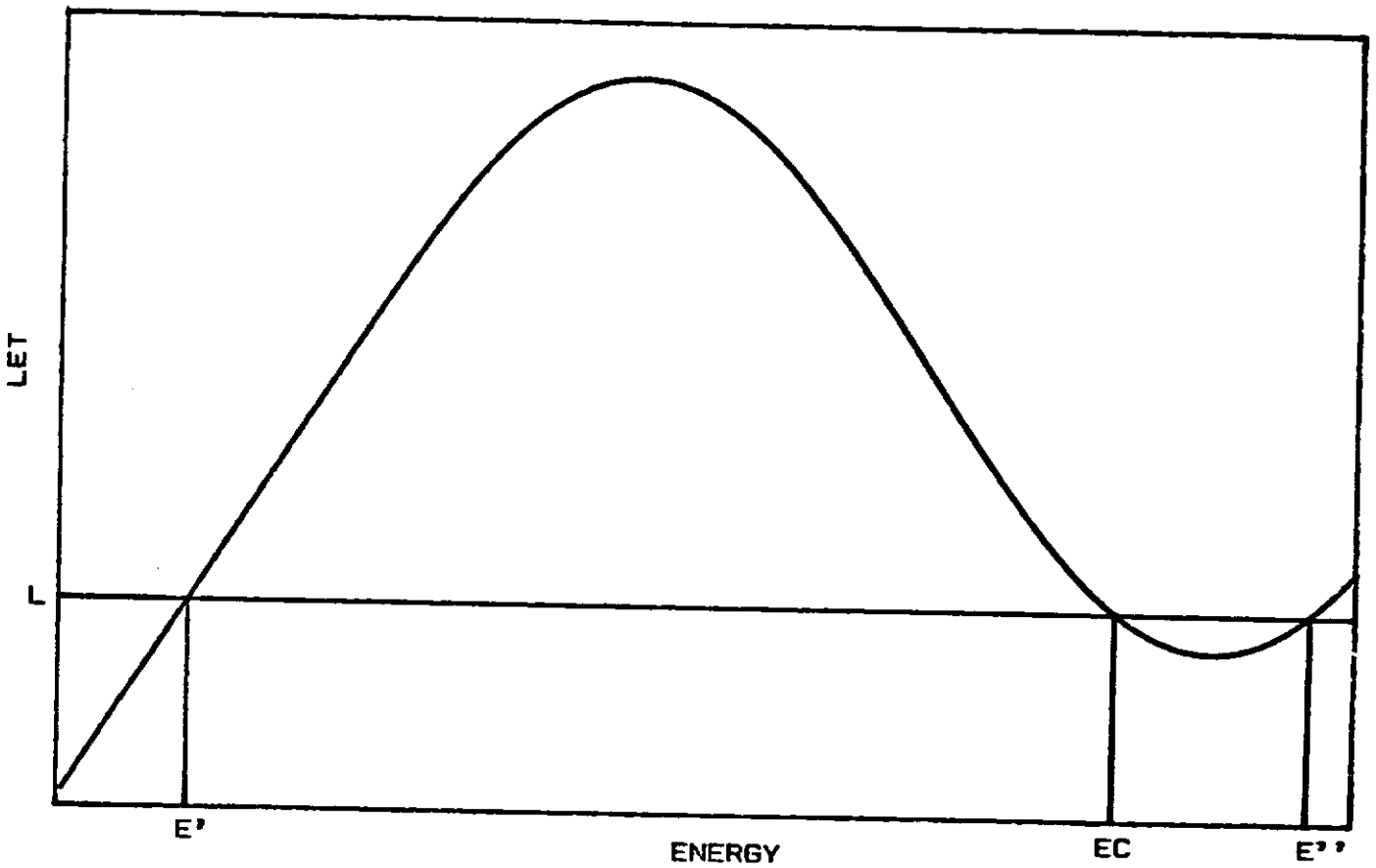

Figure 2.3. LET vs. energy curve showing typical medium cutoff EC and a special high LET denoted by L.

associated with energies under the bump. When a shield is in place, some particles will have their energies shifted to the left of the EC line and now upsets will occur. A few particles in the tail will have their energies shifted to the left of E'', thus reducing the upset rate but these very high energy particles are negligibly effected by the shield so there will be a very small number of such particles. The net result is an increase in the Heinrich Curve at this specific LET value when a shield is used. But the shield either has no effect or lowers the Heinrich Curve at the low LET values. This means the curve for the shielded case must intersect the curve for the nonshielded case at some high LET value below the value L shown in Figure 2.3.

In summary, if we compare the Heinrich Curve for a shielded case to that of the nonshielded case we can find a LET, call it LC, such that below LC the shielded curve is either the same as or lower than the nonshielded curve, and above LC the shielded curve is higher than the nonshielded curve. This is demonstrated in Figures A.4, A.5, and A.6.

HIGH MAGNETIC CUTOFF

At high cutoffs the only particles reaching the shield are at sufficiently high energies that mass shielding has a negligible effect on the spectrum (unless the shield is very thick) and, therefore, a negligible effect on the Heinrich Curves at all LETs. This is demonstrated in Figures A.1, A.2, and A.3 which show the curves for different shielding thicknesses as being indistinguishable.

Until now we have been making an oversimplification by looking at an individual species where low, medium, and high cutoffs and low and high LETs are well defined. For a mixture of species, these terms are not well defined. In particular we can, under some conditions, see a significant mixing of low LET properties with high LET properties. Let us look at a given value of LET and call it L. Let L be in the low LET interval for heavy ions. If L is in the range tabulated by UPSET FLUX, it will be in the high LET interval or above, (above meaning clear off the LET graph) for protons. Assume a very low or zero magnetic cutoff. When looking at this LET value, we are looking at heavy ions at all energies and low energy protons. Assume the worst case spectrum is not used. Then for a given species most particles are at relatively high energies and the heavy ion contribution to upsets will be affected by shielding in a way that leans towards what we would expect from high energy particles. The low energy protons are a small fraction of the total protons, but because of the abundance of protons relative to heavy ions, the low energy protons could (depending on how low is "low") be comparable in number to all of the heavy ions. So we could see characteristics expected of high energy (LET in the low interval) particles and characteristics expected of low energy (LET in the high interval) particles with comparable influences.

To further complicate things, the transmission function for a large trajectory segment (for example, a complete circular orbit) is not a simple step function. But some of the characteristics that were discussed are evident in extreme cases. For example a 0° orbital inclination, 200-km altitude orbit is so well protected by the magnetic field that it is clearly

in the high cutoff category. Shielding, using a thickness common in practice, has no effect. If a spacecraft is in the interplanetry medium, we are clearly in the low cutoff category. In this category mixing of high and low LET properties is not a complication because they both have the same properties. Shielding lowers the Heinrich Curve.

CHAPTER 3

LIMITATIONS AND SOURCES OF ERROR

In previous chapters we haven't made a distinction between what we will now call the Heinrich Flux (the quantity that is plotted in the Heinrich Curves) and the upset flux (the quantity that gives the rate that upsets occur in a part). Because actual parts are three-dimensional, the two quantities are not exactly the same. A part is not in general characterized by a single threshold LET and cross section, it is more generally characterized by a threshold LET and cross section that are functions of the arrival direction of the incident particle. Depending on the geometry of the sensitive region of the part, a threshold LET and cross section may be insensitive to arrival direction. In this case the Heinrich Flux does approximate the upset flux. For less acommodating geometries, the Heinrich Flux is still an adequate description of the environment (when the particle environment is isotropic) for predicting upset flux, given part geometry, but the procedure is more complicated than simply equating the two fluxes. The procedure is discussed in reference (6). The methods used to predict upset flux from Heinrich Flux and the associated limitations and errors will not be discussed here. What will be discussed here are the limitations and errors in the methods given in this report for calculating the Heinrich Flux.

Sources of error include errors in the calculational methods used to predict the effects of various phenomena, errors obtained by totally neglecting various phenomena, and errors in the empirical data. GEOMAG is the principal source of the errors in the first category. Because of the nature of the error introduced by GEOMAG (to be discussed below), it is not possible to make a general statement about the error that can be expected in the final Heinrich Flux calculated. The error can vary radically from case to case. The fractional error can be infinite (a zero Heinrich Flux predicted for a given LET when in fact a nonzero occurs). Although it is not possible to make a general statement about the errors that can be expected in the calculated Heinrich Flux, the limitations of the calculational methods and the conditions under which errors will be most severe can be predicted by looking at the limitations and sources of error associated with each of the individual steps in the calculation process.

GEOMAG

The limitation of GEOMAG that can produce a prediction of zero Heinrich Flux at a given LET, when in fact a nonzero value occurs, is the use of the vertical cutoff instead of a true directionally averaged cutoff. The magnetic cutoff depends on arrival direction as well as the point of observation. We can get an idea of the significance of this by referring to the STORMER CUTOFF for a simple magnetic dipole. The biggest spread in the cutoffs for the different arrival directions occurs in the dipole equatorial plane. It is not difficult to theoretically calculate the directionally averaged transmission function for the dipole. This has been calculated in the equatorial plane and plotted against rigidity in Figure 3.1. Also shown in Figure 3.1 is the vertical cutoff, denoted by PV, and the step function that GEOMAG uses to

simulate the directionally averaged transmission function. If the horizontal axis is labeled in units of PV, the plot does not depend on distance from the dipole or on the strength of the dipole moment. The rigidity where the directionally averaged transmission function first differs from zero is about 0.686 PV and this is the cutoff rigidity for the arrival direction that has the minimum cutoff. The rigidity where the directionally averaged transmission function levels off to unity is 4 PV. It is the cutoff rigidity for the arrival direction that has the maximum cutoff.

By terminating the spectrum below PV, as GEOMAG does, we are excluding some lower energy particles (particles with rigidity between 0.686 PV and 1.0 PV) that can actually reach the point of observation. This would normally introduce only a small error in the total integrated directionally averaged flux but the error introduced in the Heinrich Flux is more subtle. The end result is that particles with energies lower than predicted will reach the spacecraft. Suppose the minimum cutoff along a trajectory segment (by this we mean the vertical cutoff minimized in location) is a medium cutoff and suppose that for a given particle species it is at EC in Figure 2.3. At the value L shown in Figure 2.3 we would predict no contributions to the Heinrich Flux from particles whose energies are under the bump of the LET curve and unless some contributions come from particles in the tail of the LET curve we would predict no Heinrich Flux from that particle species at that LET value. In reality some particles with energies below EC will reach the spacecraft and the actual Heinrich Flux at this LET value will not be zero.

By looking at an individual particle species and the specific LET value just described we have intensified the error that is being discussed. Fortunately the error is less severe when looking at a mixture of particle species. It is also interesting that the error has a dependence on the trajectory segment. Reference (1) shows a comparison between the transmission function calculated by GEOMAG and a more accurately calculated (by trajectory-tracing methods) directionally averaged transmission function for a 50-degree inclination circular orbit at a 400-km altitude. The comparison is impressive. The two curves differ from zero at nearly the same location. But for a high inclination orbit, the minimum cutoff occurs at high latitudes. At high latitudes the cutoffs for different arrival directions are practically the same (at least as predicted by the dipole model), so the predicted minimum cutoff will be practically the same whether we minimize the vertical cutoff in location or we minimize the directionally dependent cutoff in both location and arrival direction. So, although this particular orbit provides an impressive demonstration of the accuracy of the transmission function calculated by GEOMAG, it does not allow us to reach general conclusions that can be applied to an arbitrary trajectory segment. A number of specific examples given in reference (1) indicate that the error is minor (probably less than the other sources of error to be discussed later) if we look at complete circular orbits with an inclination not less than 30°. The error will be most pronounced when looking at short trajectory segments near the magnetic equator. Even in this case the error in the Heinrich Flux depends on the LET value. The fractional error will be small when the Heinrich Flux is large.

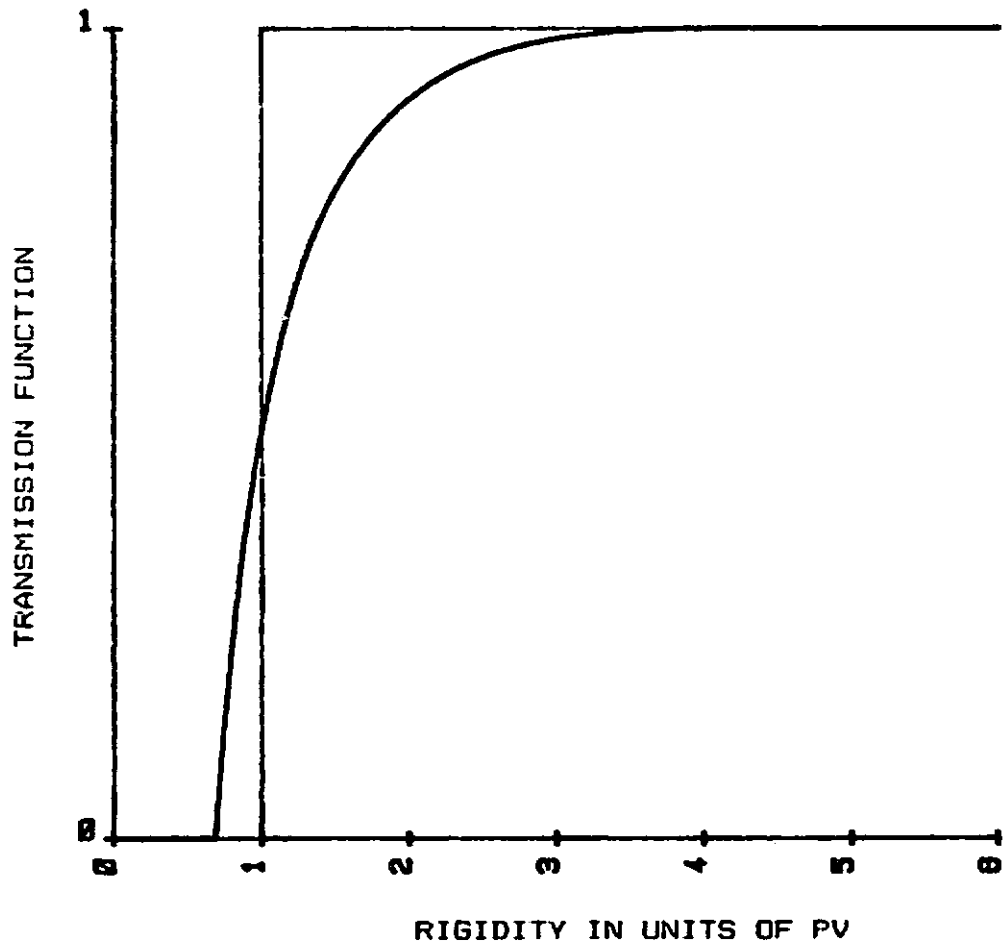

Figure 3.1. The directionally averaged transmission function, applicable to a magnetic dipole, evaluated at a point in the dipole's equatorial plane. The horizontal axis is labelled in units of vertical cutoff rigidity. Also shown is the step function that GEOMAG would use to simulate the smooth curve.

SPECTRUM

As of 1983 there was still much uncertainty about the anomalous component (see reference (1)); therefore, it has not been included. The anomalous component affects nitrogen and oxygen only up to about 30 MeV/nucleon and this is easily blocked by magnetic shielding or mass shielding. Helium is affected up to 200 MeV/nucleon which is more difficult to block with mass shielding. But a radiation hard part with a minimum threshold LET (minimized in arrival direction) above 2 MeV-cm^2/mg will not see upsets from these ions by direct ionization. If it is suspected that the anomalous component will affect the mission of the spacecraft, it will have to be treated separately.

We do not have adequate information on the cosmic ray spectra below 10 MeV/nucleon. Unless the geomagnetic cutoff blocks all such particles, meaningful results can be obtained ony behind a shield thick enough to stop all particles with energies less than 10 MeV/nucleon. The computer programs will run if a thinner shield is used, but the outputs will be the same as they would be if the differential interplanetary flux were zero below 10 MeV/nucleon.

SPECTRUM does not include ions with atomic numbers greater than 28. Because of their scarcity, these very heavy ions will not be a dominant source of upsets if lighter ions can cause upsets. If a part is so radiation hard that atomic numbers less than or equal to 28 will not cause upsets, the heavier ions must be included to obtain even a low order approximation to the upset rate.

Reference (2) states that the probable errors in the data that are contained in SPECTRUM have a dependence on energy, particle species, and type of solar modulation (whether it be solar minimum or solar maximum). The prediction of future levels of solar modulation appears to be the major source of error in predicting the cosmic ray spectra. This alone can lead to errors of about a factor of 5 for some species at some energies. This was the most pessimistic figure for an error given in reference (2) with the exception of low energy iron. There are very few experimental data for low energy iron, and the low energy part of the spectrum is essentially an extrapolation. The reader is referred to reference (2) for details.

TRANSPORT

TRANSPORT considers only uniform spherical shields with the point of observation being at the center of the shield. Bremsstrahlung, straggling, and all nuclear reactions between an incident particle and the shield material are neglected. An analysis of these phenomena is beyond the scope of this report and an associated error estimate in the Heinrich Curves will not be given.

It is assumed that the errors that have not been mentioned above, including errors in the numerical methods, are minor compared to the errors that have been mentioned above.

In closing we would like to mention that an indication that we should be concerned with the errors and limitations that were just described is the prediction of zero or a very low Heinrich Flux. Although, we could probably expect upset rates to be small (in some sense of the word "small") we must be careful. GEOMAG could estimate a cutoff to be too high, or a phenomena (e.g., spallation) or an aspect of the environment that was neglected (e.g., ions heavier than nickel) may be the dominant source of upsets.

REFERENCES

1. Adams, J.H. Jr., Letaw, J.R., and Smart, D.F., "Cosmic Ray Effects on Microelectronics, Part II: The Geomagnetic Cutoff Effects," NRL Memorandum Report 5099, May 26, 1983.

2. Adams, J.H. Jr., Silberberg, R., and Tsao, C.H., "Cosmic Ray Effects on Microelectronics, Part 1: The Near-Earth particle Environment," NRL Memorandum Report 4506, August 25, 1981.

3. Shea, M.A., and Smart, D.F., Report No. AFCRL-TR-75-0185, Hanscom, AFB, Mass., 1975.

4. Johnson, F.S., Satellite Environment Handbook, Stanford University Press, Stanford, California, 1965.

5. Northcliffe, L.C., and Schilling, R.F., "Range and Stopping Power Tables for Heavy Ions," Nuclear Data Tables, A7233-463 (1970), Academic Press, 1970.

6. Tsao, C.H., Silberberg, R., Adams, J.H. Jr., and Letaw, J.R., "Cosmic Ray Effects on Microelectronics, Part III: Propagation of Cosmic Rays in the Atmosphere," NRL Memorandum Report 5402, August 9, 1984.

7. Jones, F.C., "Cosmic-Ray Modulation and the Anomalous Component," Reviews of Geophysics and Space Physics, Vol. 21, No. 2, March 1983.

8. Rossi, B., and Olbert, S., Introduction To the Physics of Space, McGraw-Hill, 1970.

APPENDIX A

EXAMPLES

The following plots are an organized listing of Heinrich Curves that may be useful for rough estimates of the Heinrich Curve for an arbitrary circular orbit. The examples cover all combinations of orbital inclination = 0, 30°, 45°, 60°, and 90°, altitude = 200 km and 1000 km. For orbital inclinations less than or equal to 45°, the minimum geomagnetic cutoff is sufficiently high that it makes no difference whether or not the worst case, low energy spectra are used. For inclinations of 60° and 90°, plots are given with and without the worst case spectra. Plots applicable to interplanetary space with and without the worst case spectra are also given. Several shielding thicknesses are used. The numbers adjacent to the curves are the shielding thickness in mm of aluminum.

The number of time steps for these plots was chosen so that the plots represent a time average over a 2-day period. The date of the orbit was chosen so that the curves represent solar minimum.

The flux plotted is one fourth of the omnidirectional flux, i.e., it is the rate per area that particles cross a surface element.

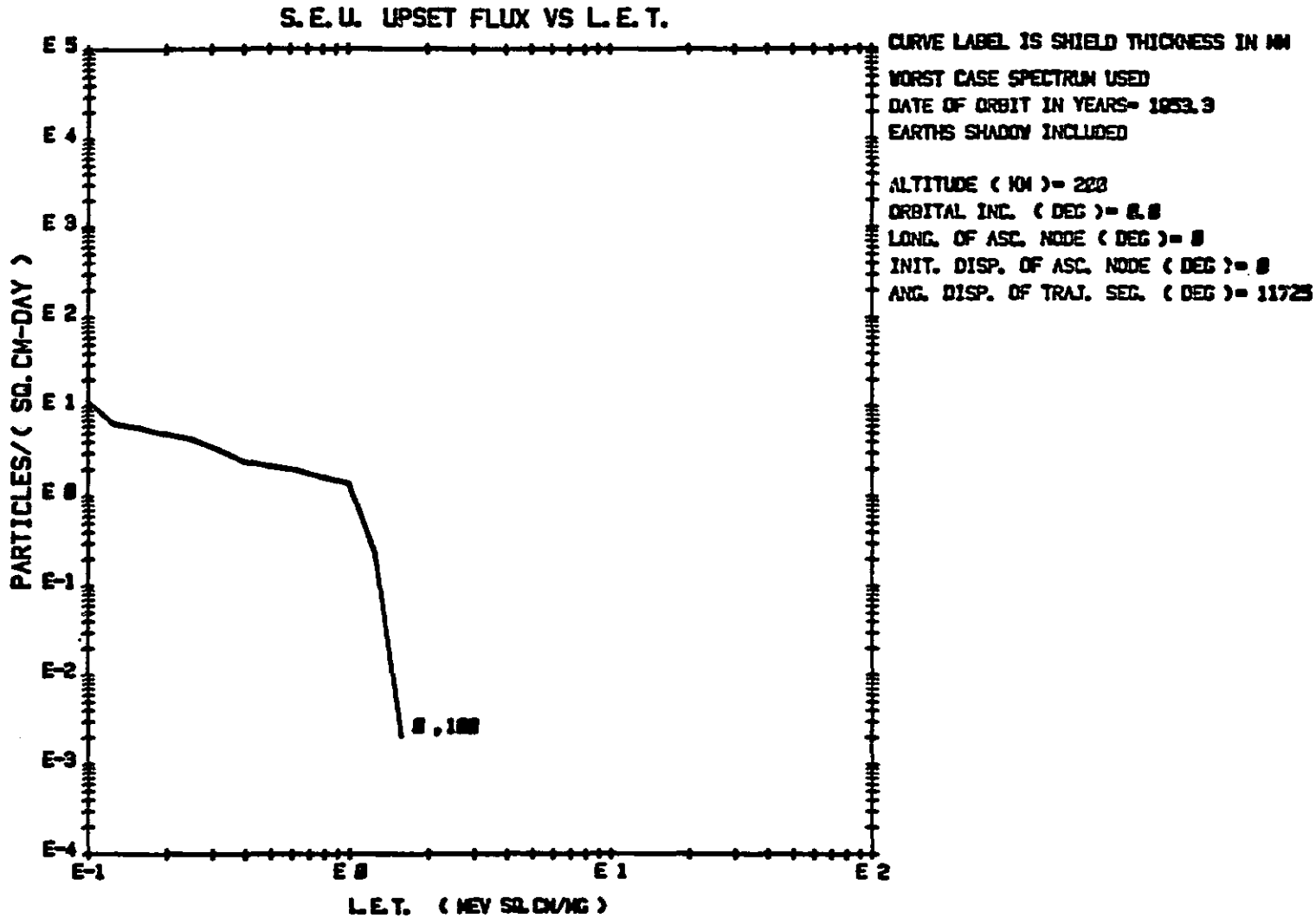

FIG. A.1. HEINRICH CURVE FOR 0 DEG. INCLINATION, 200 KM ALTITUDE ORBIT. WORST CASE SPECTRUM USED

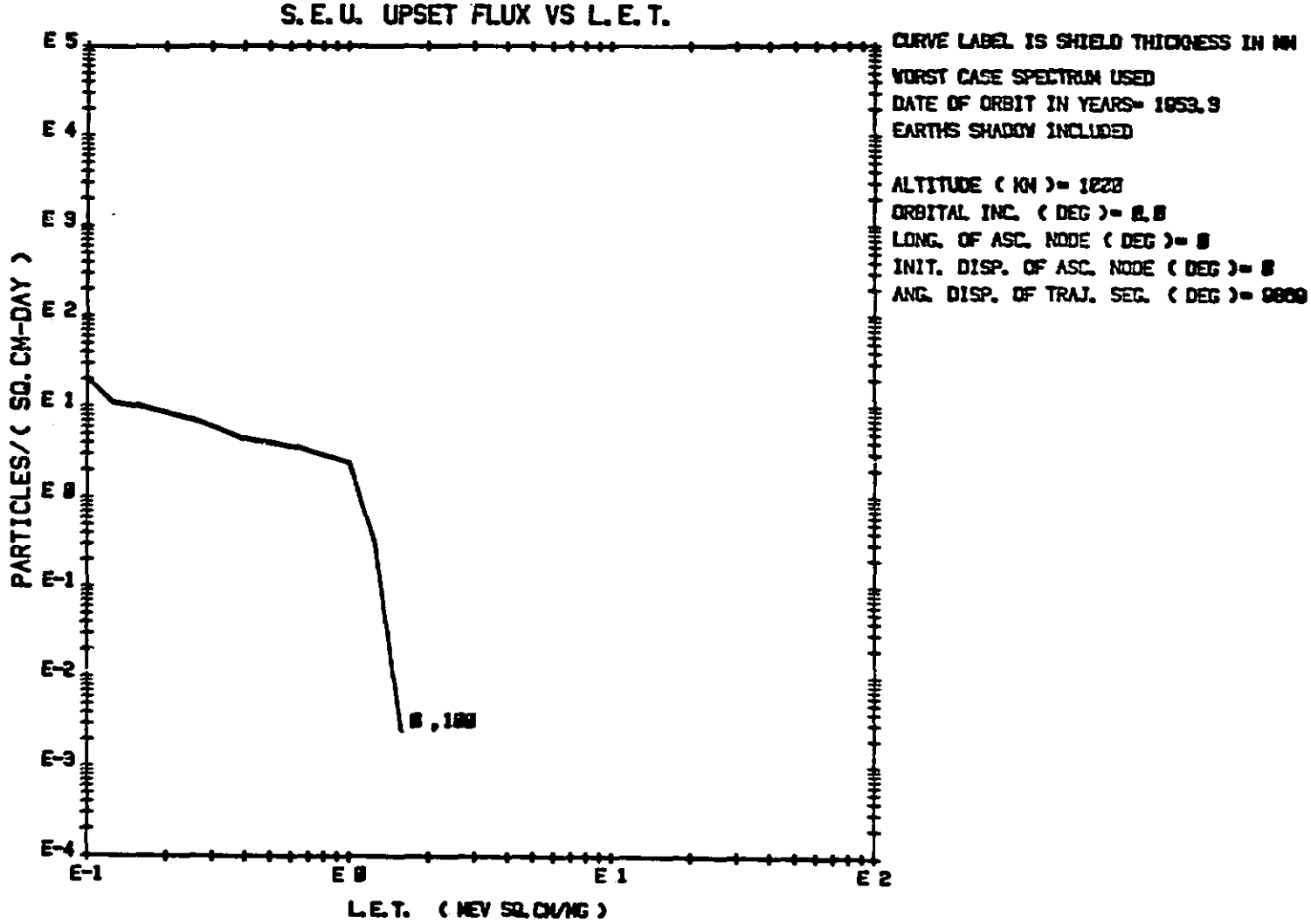

FIG. R.2. HEINRICH CURVE FOR 0 DEG. INCLINATION, 1000 KM ALTITUDE ORBIT. WORST CASE SPECTRUM USED

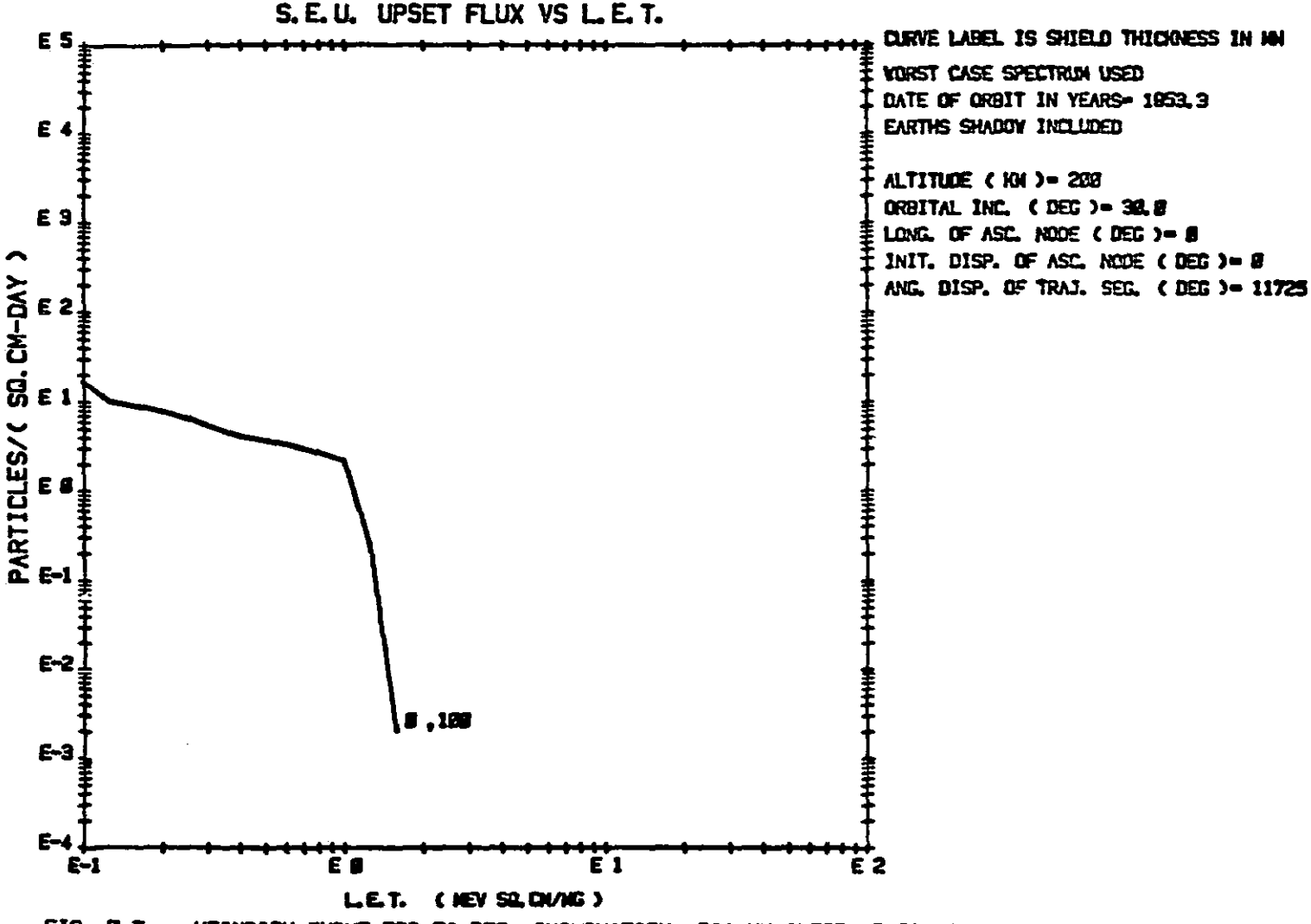

FIG. A.3. HEINRICH CURVE FOR 30 DEG. INCLINATION, 200 KM ALTITUDE ORBIT. WORST CASE SPECTRUM USED

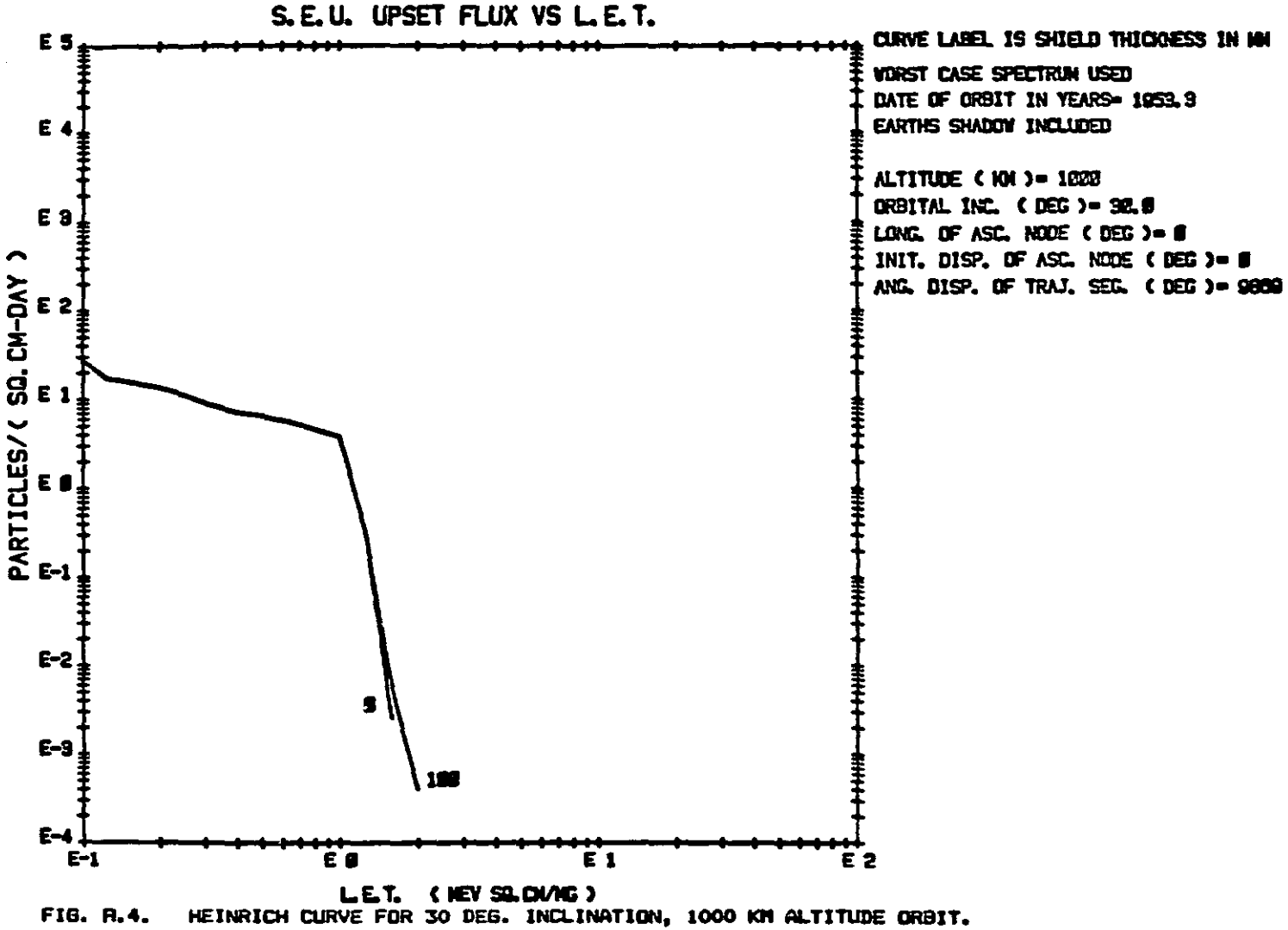

FIG. A.4. HEINRICH CURVE FOR 30 DEG. INCLINATION, 1000 KM ALTITUDE ORBIT. WORST CASE SPECTRUM USED

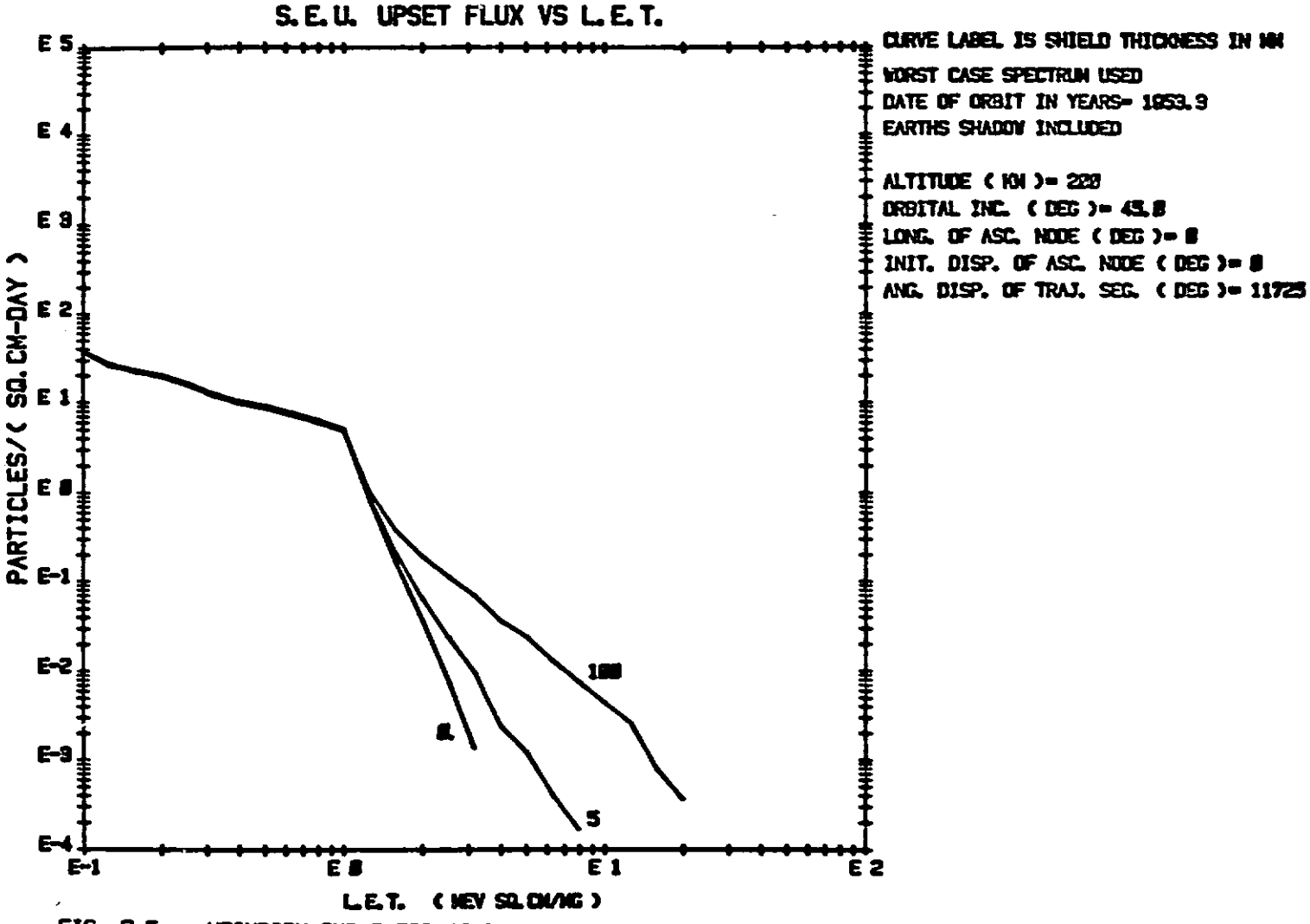

FIG. A.5. HEINRICH CURVE FOR 45 DEG. INCLINATION, 200 KM ALTITUDE ORBIT. WORST CASE SPECTRUM USED

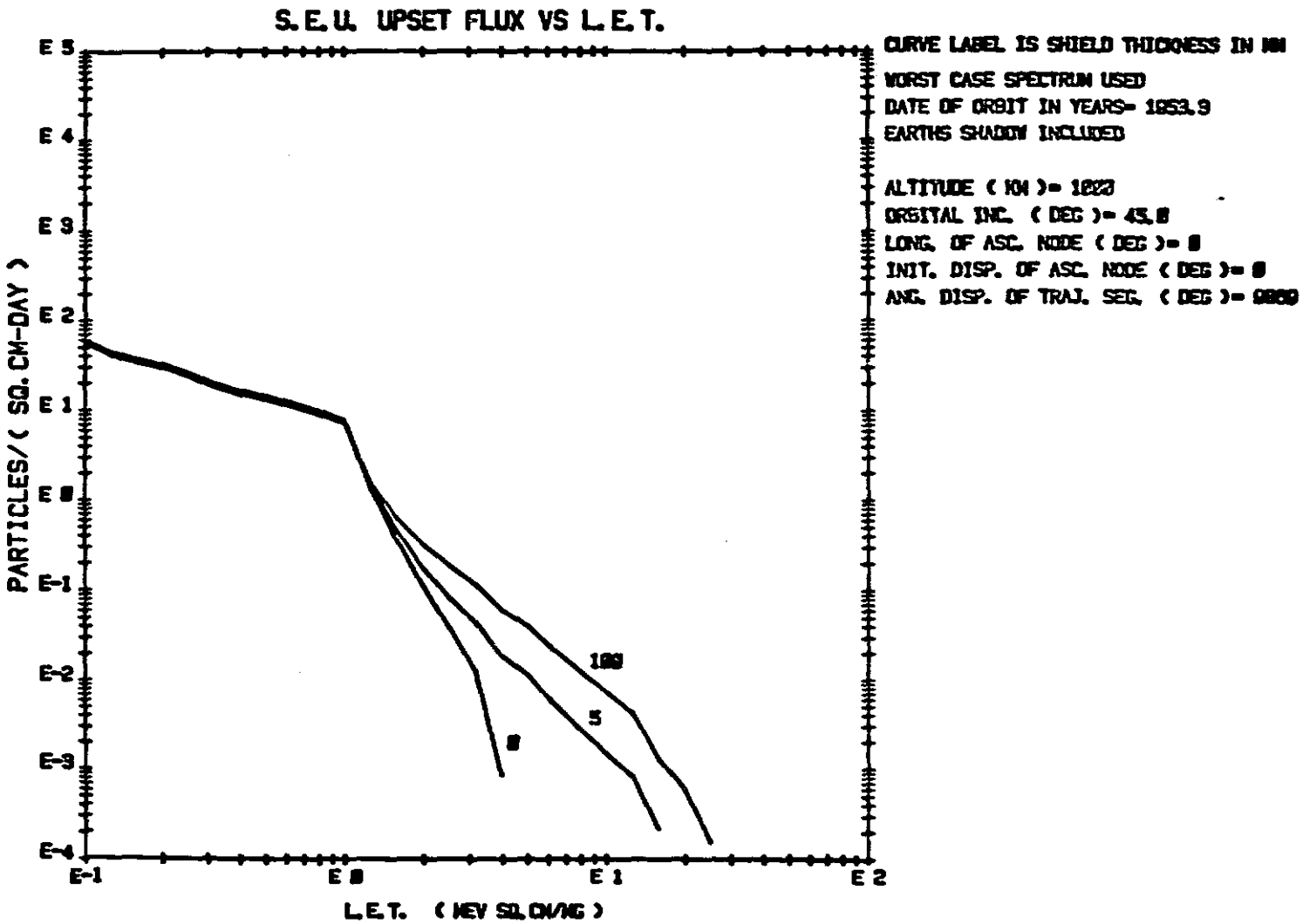

FIG. A.6. HEINRICH CURVE FOR 45 DEG. INCLINATION, 1000 KM ALTITUDE ORBIT, WORST CASE SPECTRUM USED

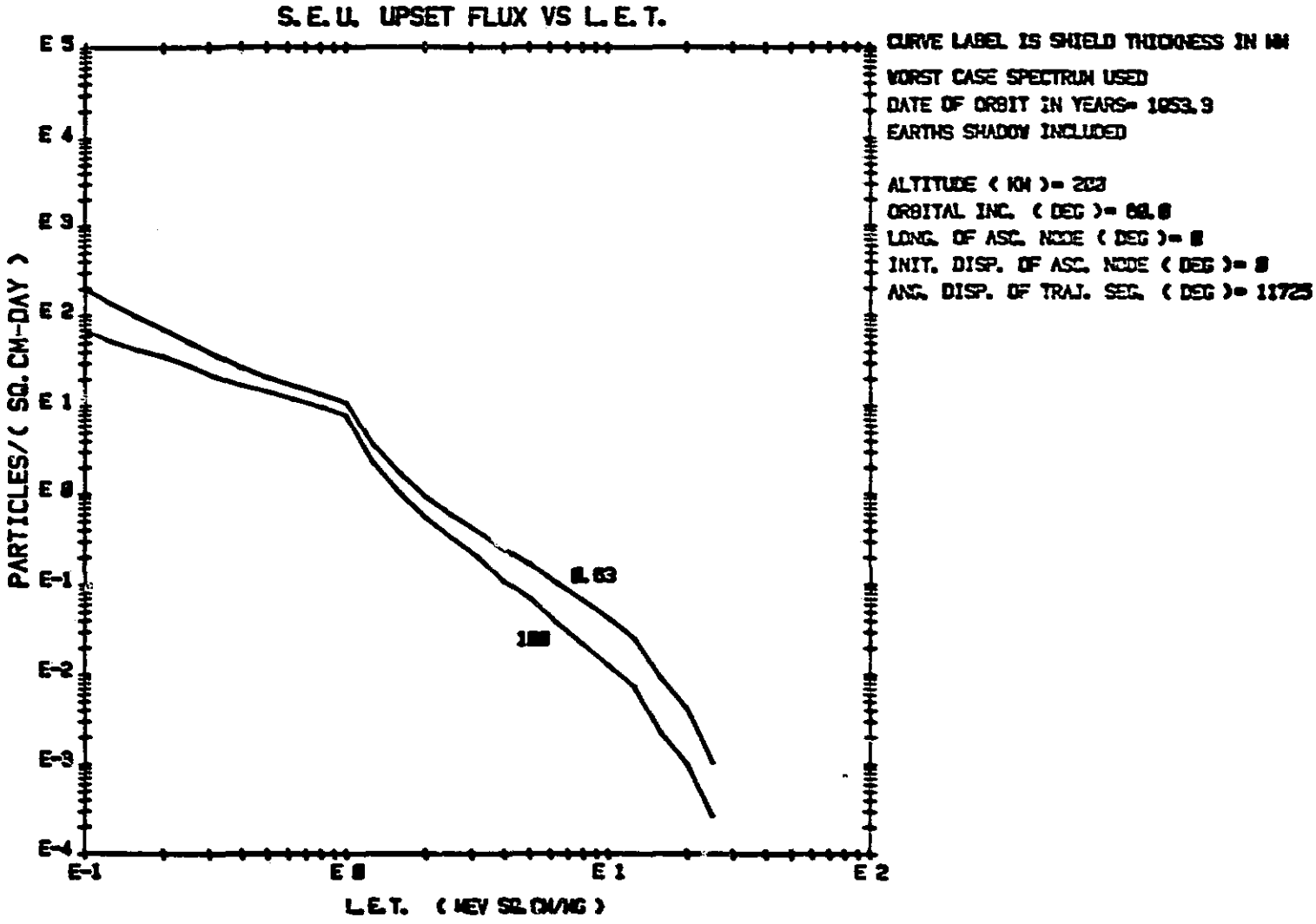

FIG. A.7. HEINRICH CURVE FOR 60 DEG. INCLINATION, 200 KM ALTITUDE ORBIT. WORST CASE SPECTRUM USED

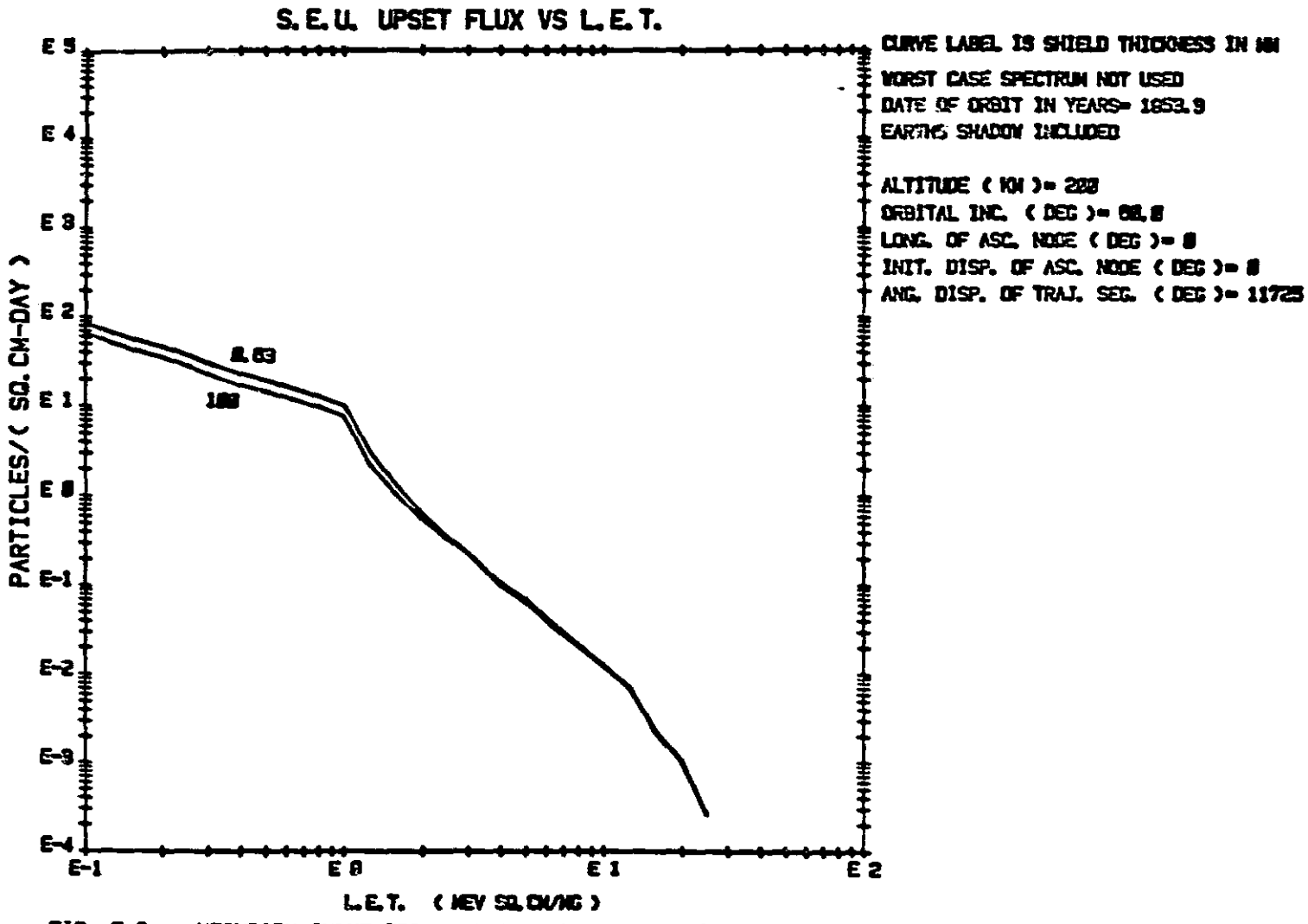

FIG. A.8. HEINRICH CURVE FOR 60 DEG. INCLINATION, 200 KM ALTITUDE ORBIT. WORST CASE SPECTRA NOT USED

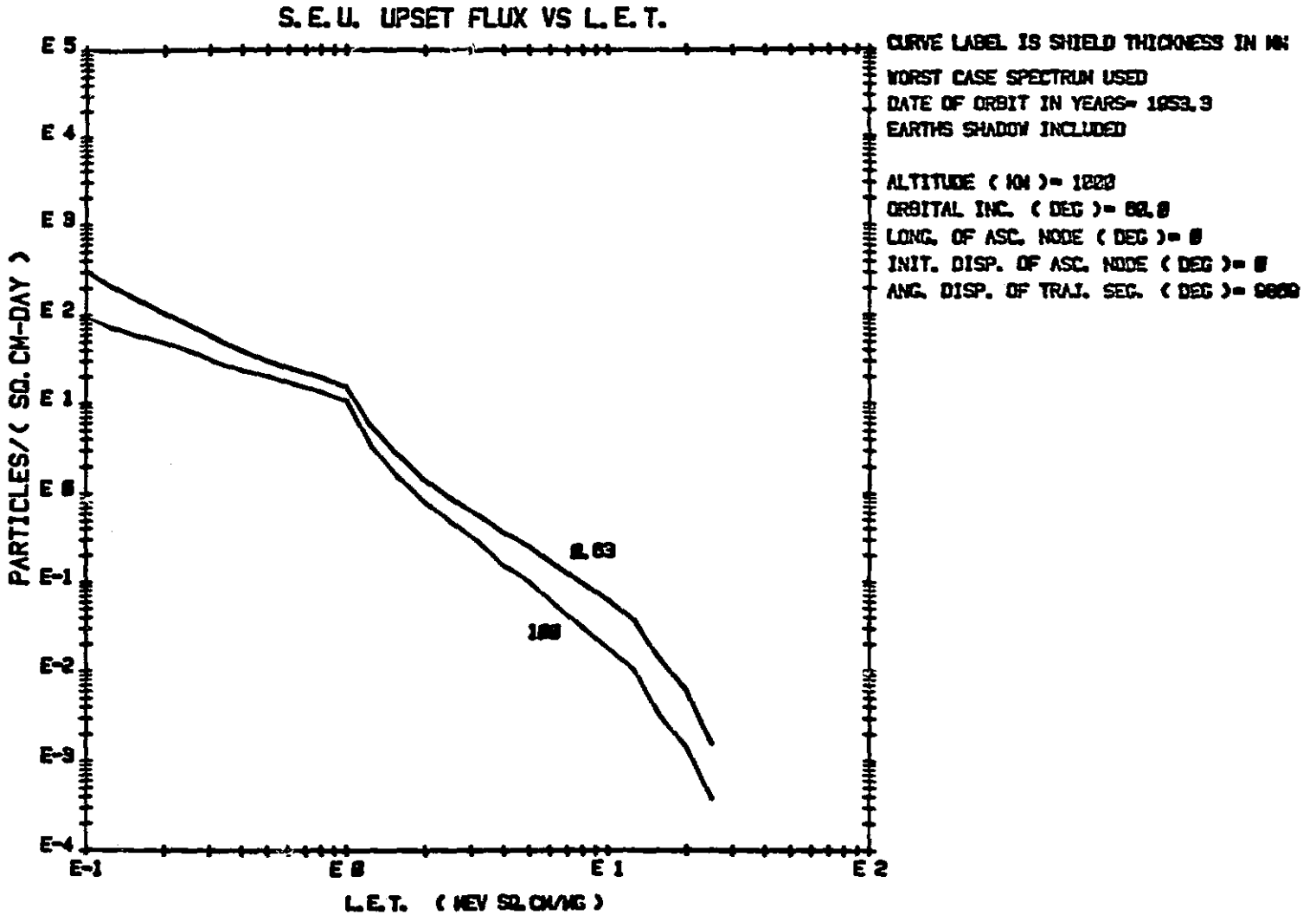

FIG. A.9. HEINRICH CURVE FOR 60 DEG. INCLINATION, 1000 KM ALTITUDE ORBIT. WORST CASE SPECTRUM USED

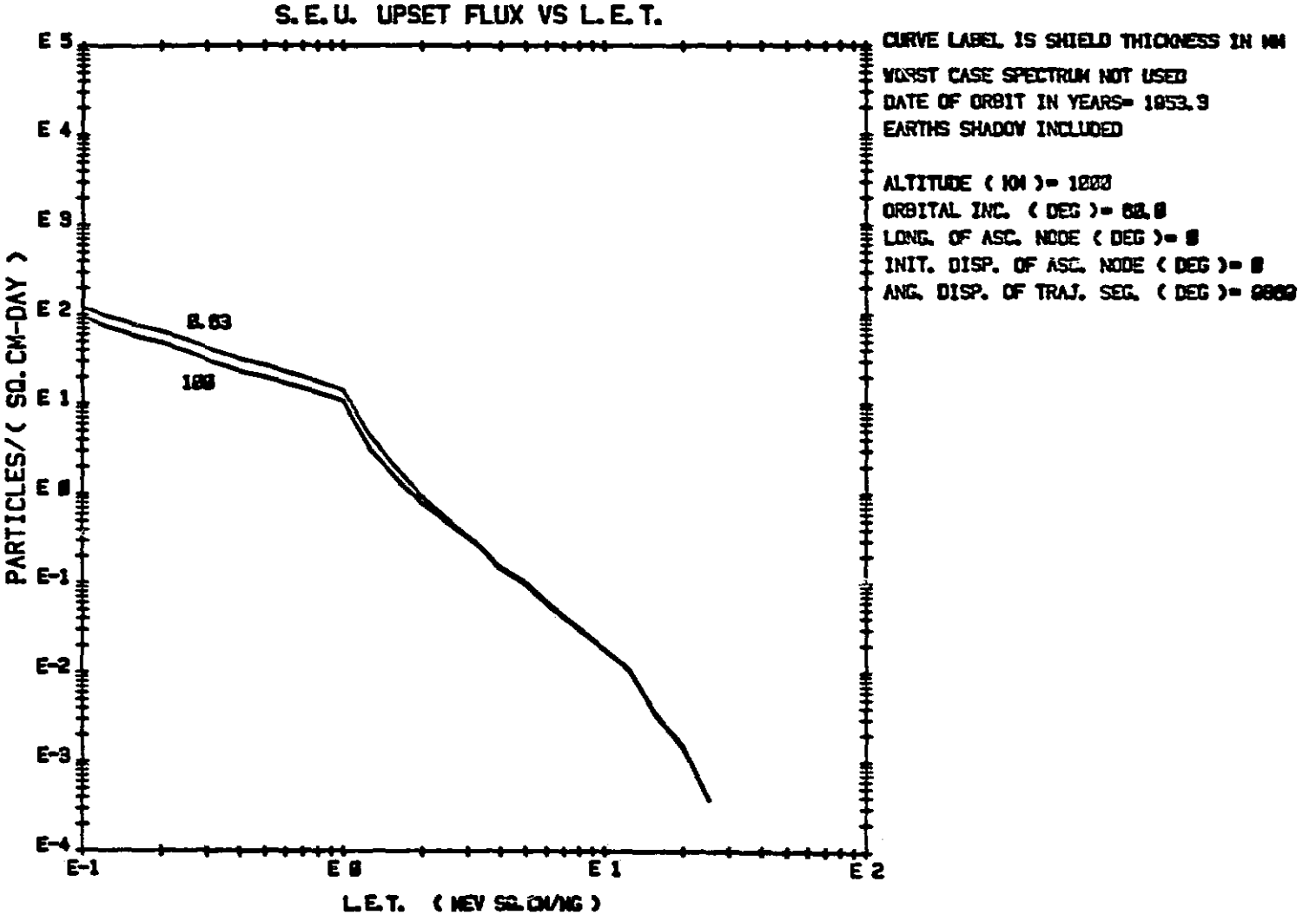

FIG. A.10. HEINRICH CURVE FOR 60 DEG. INCLINATION, 1000 KM ALTITUDE ORBIT. WORST CASE SPECTRA NOT USED

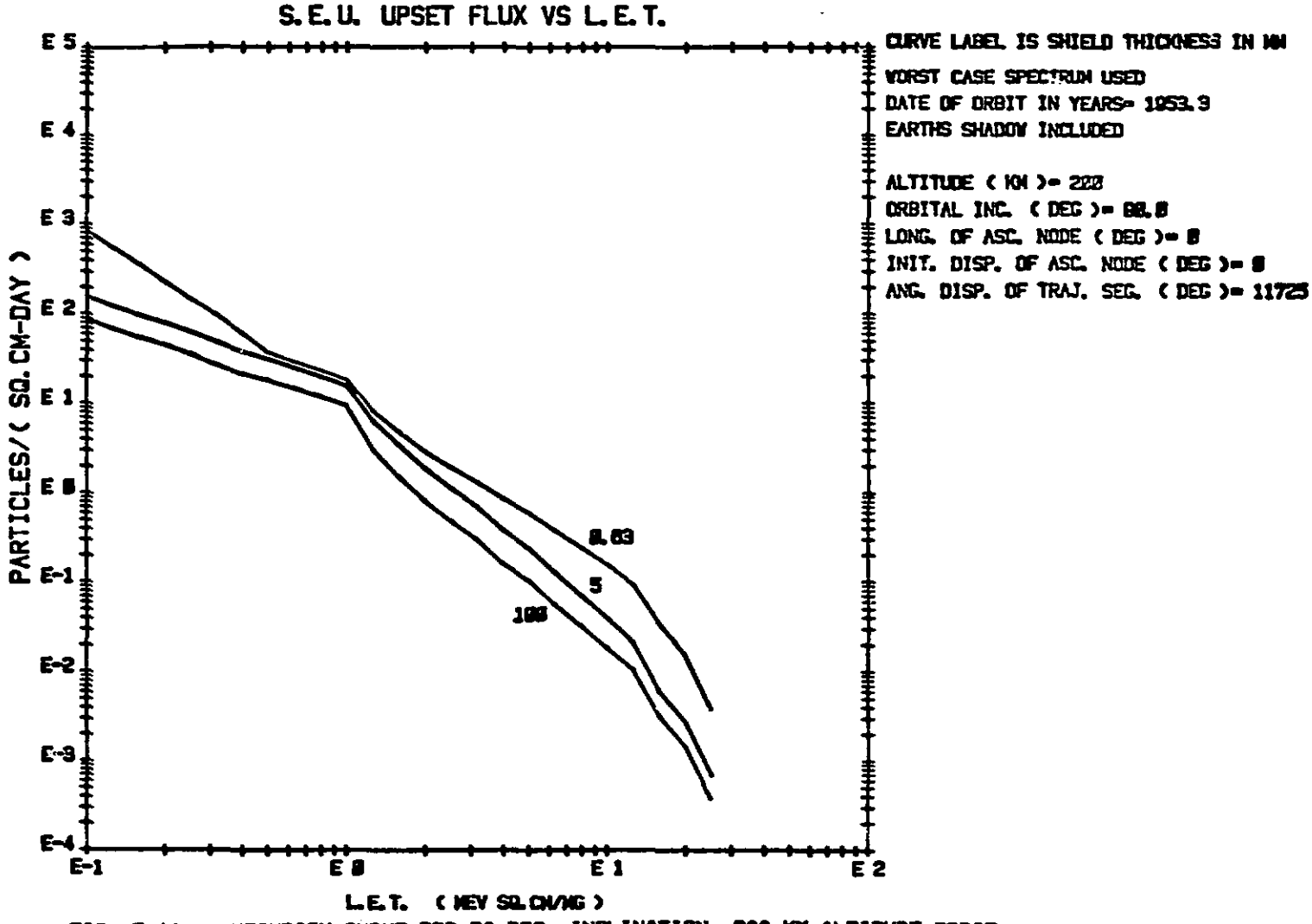

FIG. A.11. HEINRICH CURVE FOR 90 DEG. INCLINATION, 200 KM ALTITUDE ORBIT. WORST CASE SPECTRUM USED

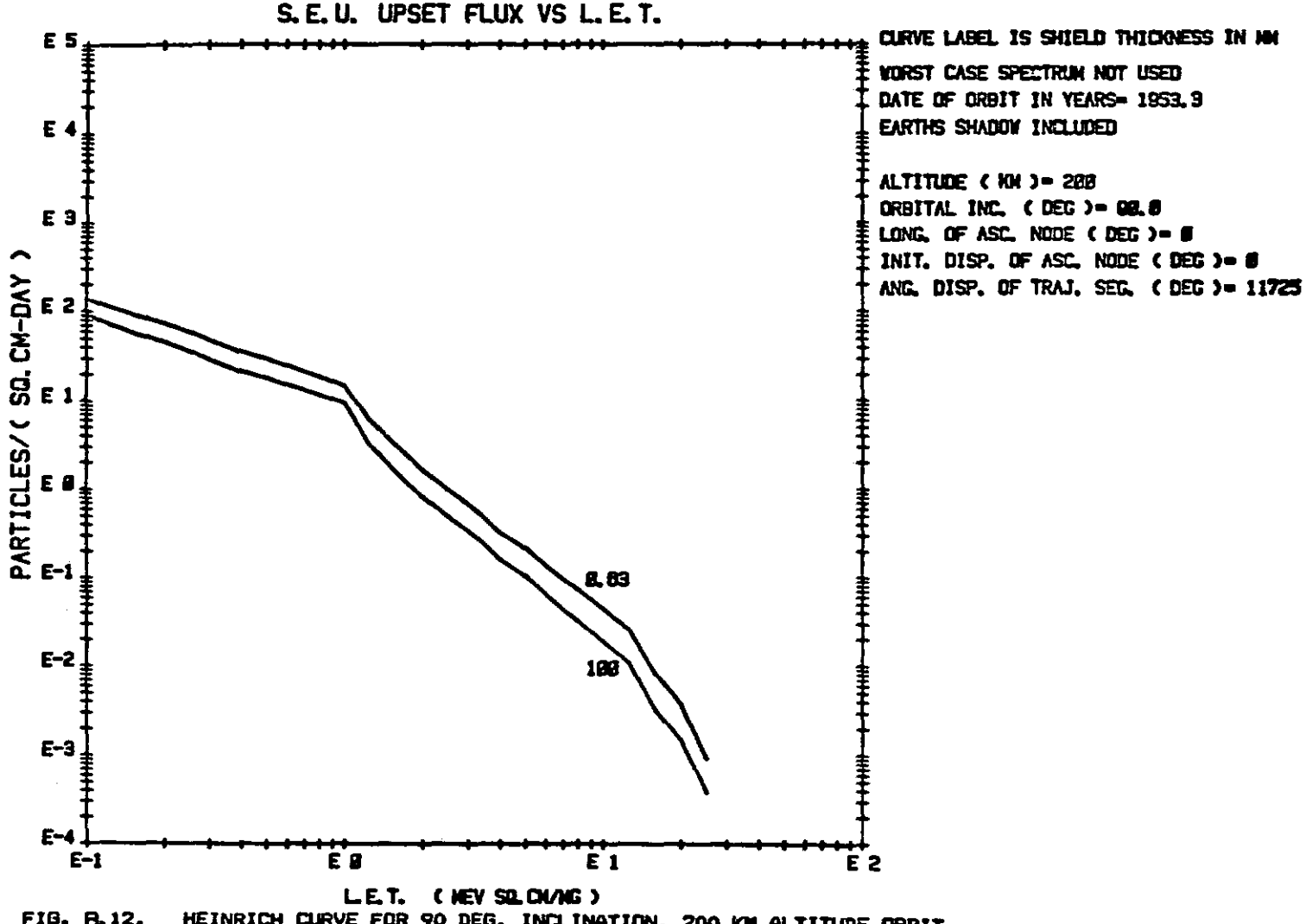

FIG. R.12. HEINRICH CURVE FOR 90 DEG. INCLINATION, 200 KM ALTITUDE ORBIT. WORST CASE SPECTRA NOT USED

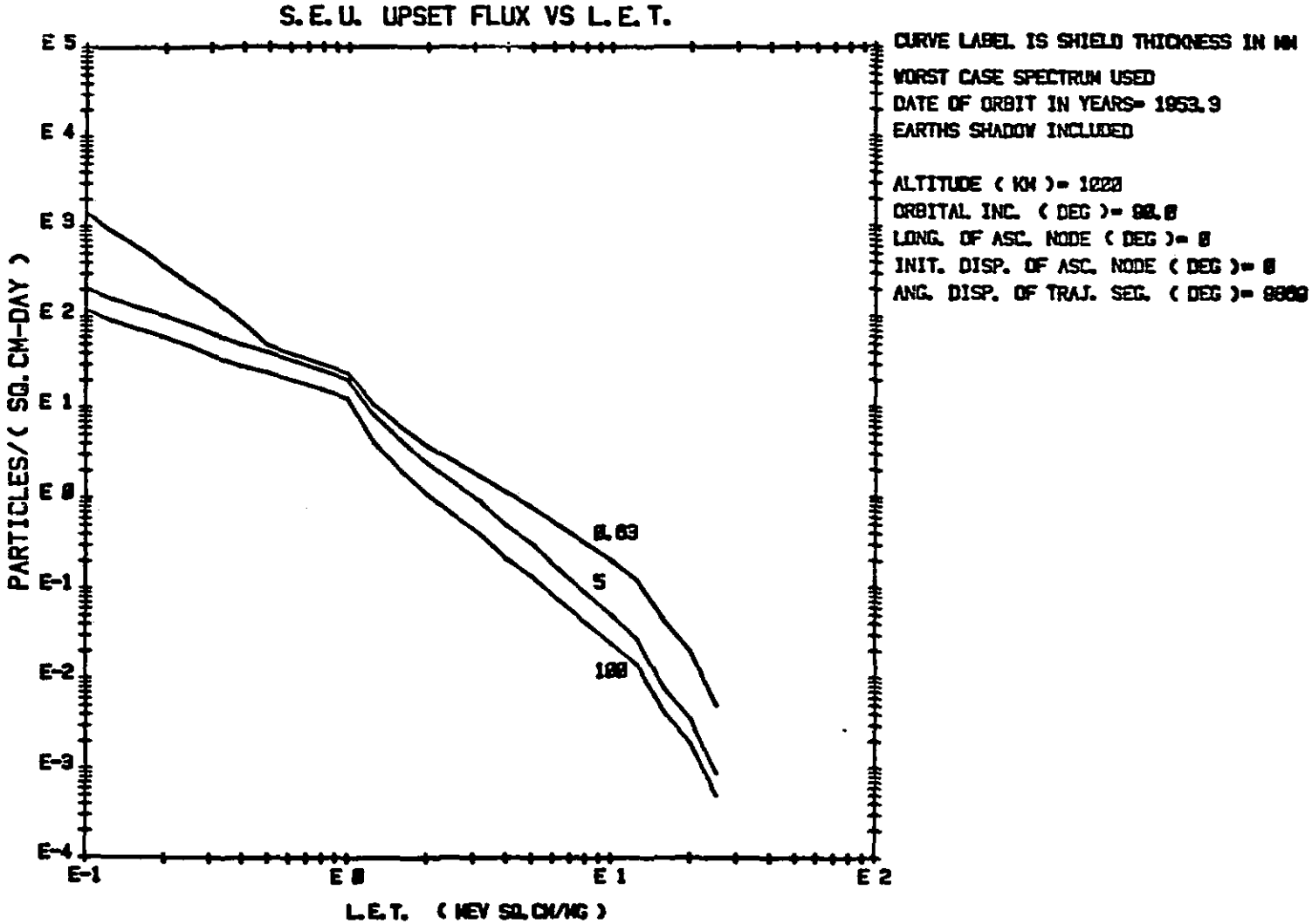

FIG. A.13. HEINRICH CURVE FOR 90 DEG. INCLINATION, 1000 KM ALTITUDE ORBIT. WORST CASE SPECTRUM USED

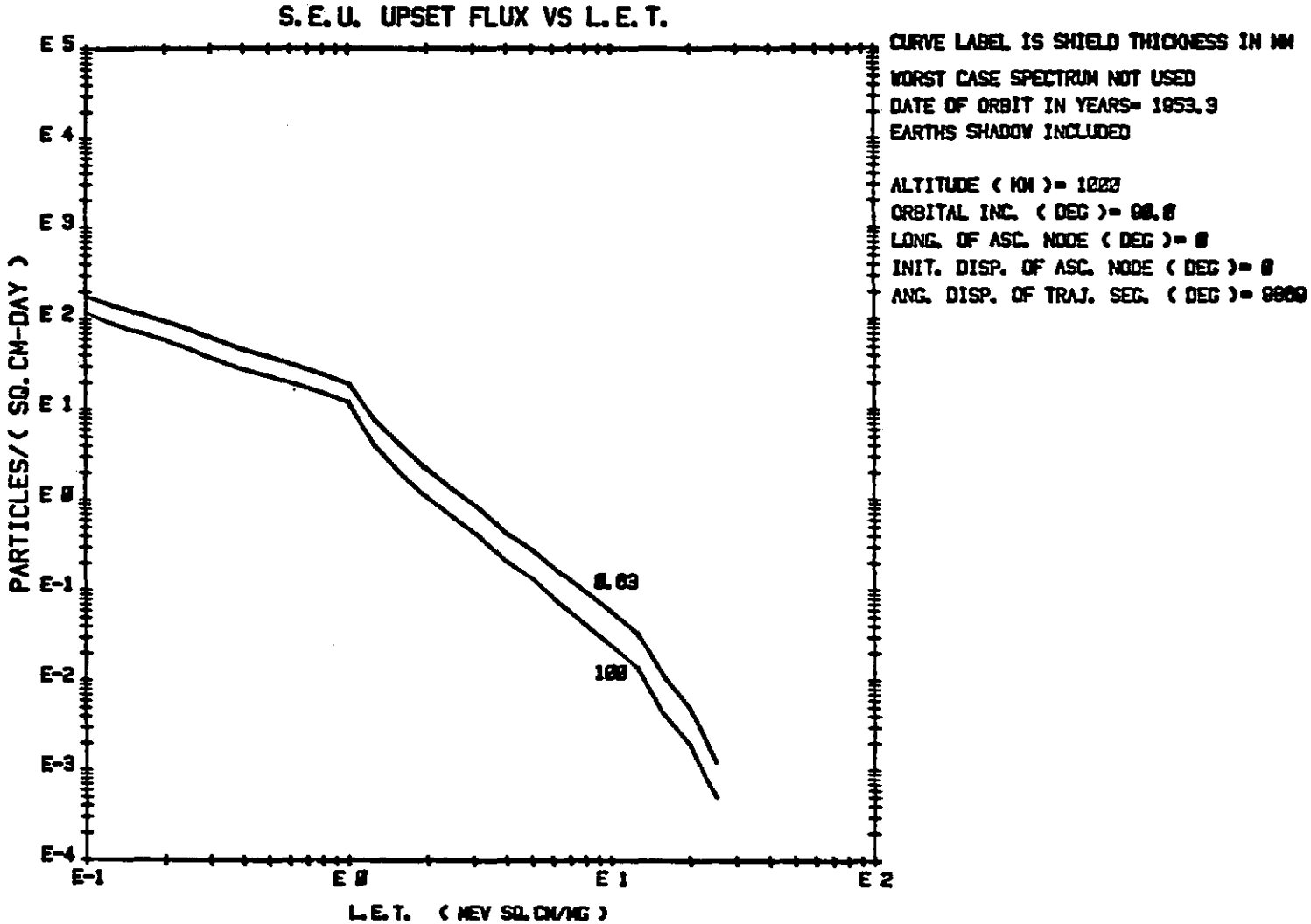

FIG. A.14. HEINRICH CURVE FOR 90 DEG. INCLINATION, 1000 KM ALTITUDE ORBIT. WORST CASE SPECTRA NOT USED

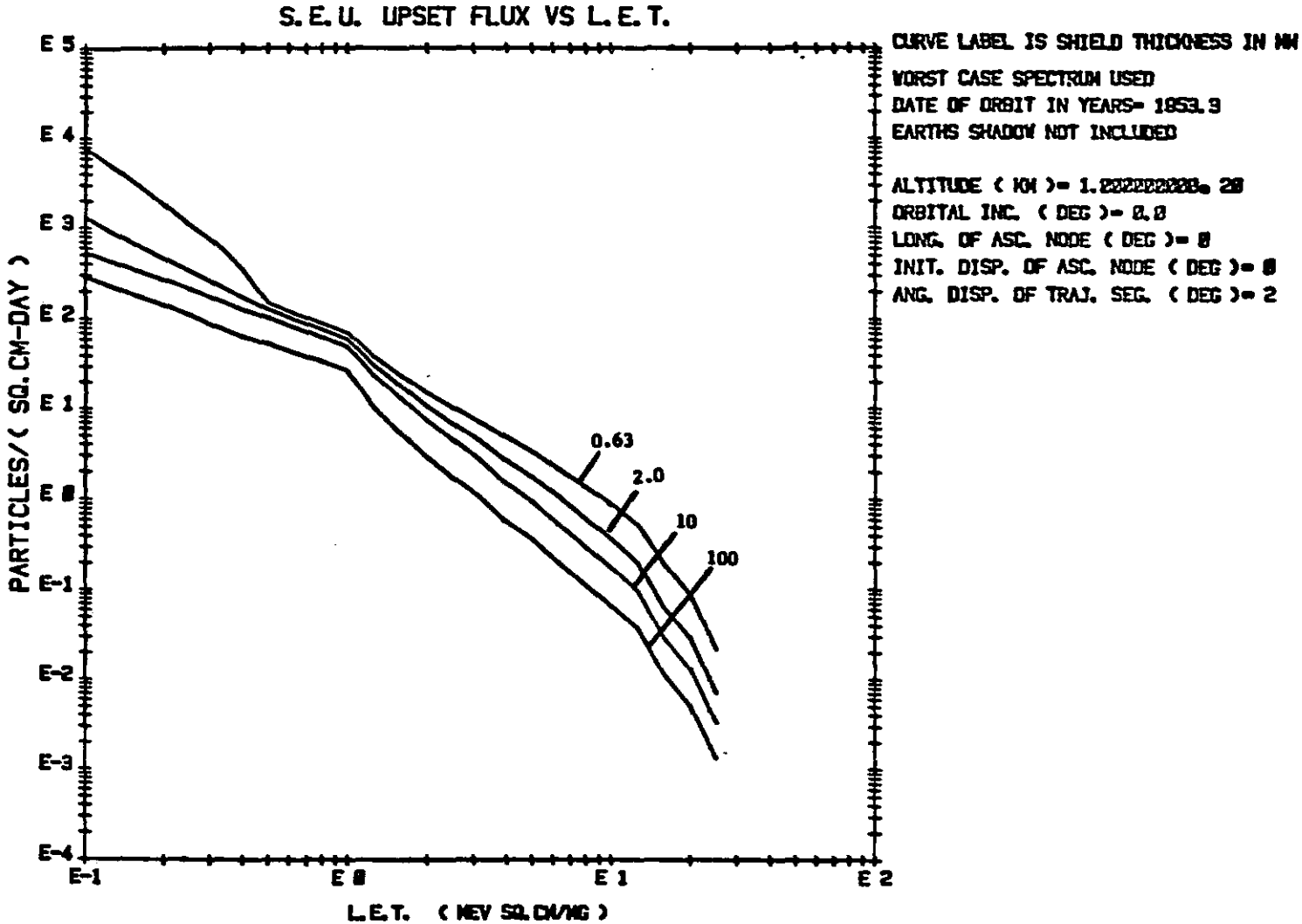

FIG. A.15. HEINRICH CURVE FOR INTERPLANETARY SPACE. WORST CASE SPECTRA USED

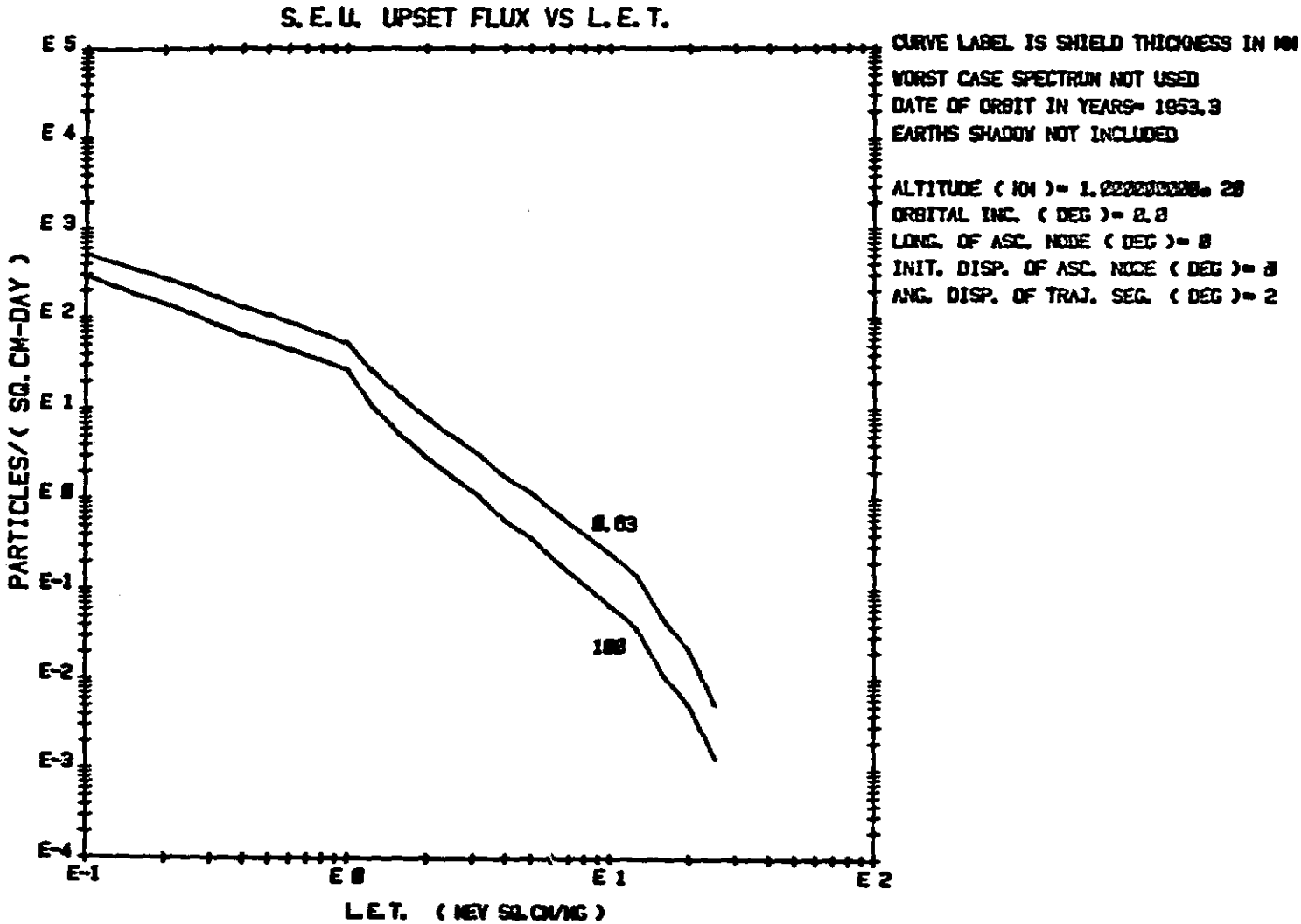

FIG. A.16. HEINRICH CURVE FOR INTERPLANETARY SPACE. WORST CASE SPECTRA NOT USED

APPENDIX B

DERIVATION OF THE EFFECTS OF MASS SHIELDING ON PARTICLE FLUX

For a given point of evaluation $\vec{x}$, arrival direction given by $\vec{n}$, and energy E, let J $(\vec{x},\vec{n},E)$ represent the differential directional intensity for a given particle species. J represents a number of particles per area per time per solid angle per energy. Let I be the energy integral of J so that

$$I(\vec{X},\vec{n},E) = \int_{E}^{\infty} J(\vec{X},\vec{n},E')dE' \tag{G1}$$

Let E_1 be an arbitrary value of energy and let $\vec{X}_1$ represent an arbitrary location in a material medium. For simplicity we assume the medium to be homogeneous although it is not hard to generalize. Let $\vec{X}_2$ represent another location in this medium with the property that the direction from $\vec{X}_1$ to $\vec{X}_2$ is parallel to $\vec{n}$. Suppose a particle is travelling from $\vec{X}_1$ to $\vec{X}_2$. Let E_2 be the energy it would have when found at $\vec{X}_2$ if it had energy E_1 when at $\vec{X}_1$. If L is the distance between $\vec{X}_1$ and $\vec{X}_2$ and R is the range function, the energies are related by

$$L = R(E_1) - R(E_2) \tag{G2}$$

or

$$E_2 = R^{-1}(R(E_1) - L) \tag{G3}$$

The relationship we have been using is

$$I(\vec{X}_1,\vec{n},E_1) = I(\vec{X}_2,\vec{n},E_2) \tag{G4}$$

If we were dealing with one dimensional geometries and we did not multiply I by a solid angle to obtain a number of particles, Equation (G4) would be an intuitively obvious consequence of conservation of particles. But since we are dealing with three dimensions and we do have to multiply by a solid angle, the relationship is perhaps less obvious. A formal derivation is given below.

Let f be the distribution function in phase space for the particle species considered. The phase space momentum coordinates will refer to ordinary linear momentum (we cannot work with momentum conjugate to the position coordinates because, as will be seen later, we will be working with forces that are velocity dependent and nonconservative). We can obtain a differential equation for f without having to resort to the Boltzmann equation with its collision terms, if we can simulate the effects of collisions with the atoms of the medium with a long range (i.e., macroscopic) force. To the extent that straggling can be neglected we can simulate the influence of the medium with a macroscopic force that is similar to a viscous force. It is opposite in direction to the particle velocity and its magnitude is governed by the particle energy and can be determined by the range function. Let F(E) denote the magnitude of this force. F is the LET of the particle, i.e., it is

the negative of the spatial rate of change of the particle's energy. The well known relationship between LET and the range function produces

$$F(E) = \frac{1}{R'(E)} \tag{G5}$$

with the prime denoting derivative with respect to E. A relationship that we will need later is obtained by taking the differential of equation (G2) by giving an independent change to E_1 while holding $\vec{X}_1$ and $\vec{X}_2$ fixed; i.e., while holding L constant. This produces

$$R'(E_1)dE_1 - R'(E_2)dE_2 = 0$$

Combining this with (G5) produces

$$\frac{dE_1}{dE_2} = \frac{F(E_1)}{F(E_2)} \tag{G6}$$

It should be emphasized that the differentials on the left side of equation (G6) are obtained by varying the initial energy of the particle (the energy at $\vec{X}_1$) while holding L fixed.

Let $\vec{v}$ represent the velocity of the particle with v the magnitude of $\vec{v}$ and let $\vec{\nabla}_x$ and $\vec{\nabla}_p$ be the del operators in position and momentum space respectively. Let $\vec{F} = -F\,\vec{v}/v$ be the force vector acting on the particle. The equation governing the distribution function can be found in reference (8) and it is

$$\vec{v} \circ \vec{\nabla}_x f + f\,\vec{\nabla}_p \circ \vec{F} + \vec{F} \circ \vec{\nabla}_p f = 0$$

which can be rewritten as

$$\vec{v} \circ \vec{\nabla}_x f - \vec{\nabla}_p \circ (fF\vec{v}/v) = 0$$

If we use the differential identity

$$\vec{\nabla}_p \circ (fF\vec{v}/v) = \frac{1}{p^2}\frac{\partial}{\partial P}(P^2 fF)$$

together with the fact that P and F are constants when operated on by $\vec{\nabla}_x$ we produce

$$\vec{v} \circ \vec{\nabla}_x (FP^2 f) - F\frac{\partial}{\partial P}(FP^2 f) = 0$$

But

$$\vec{F} \circ \vec{\nabla}_p = - F \frac{\partial}{\partial P}$$

so we finally obtain

$$\vec{v} \circ \vec{\nabla}_x (FP^2 f) + \vec{F} \circ \vec{\nabla}_p (FP^2 f) = 0 \qquad (G7)$$

Equation (G7) is a statement that the convective derivative of $FP^2 f$ is zero which implies that $FP^2 f$ is constant on a particle trajectory. We therefore have

$$F(E_2)\, P_2^2\, f(\vec{x}_2, \vec{n}, P_2) = F(E_1)\, P_1^2\, f(\vec{x}_1, \vec{n}, P_1) \qquad (G8)$$

where P_1 and P_2 are the momentums of the particle at $\vec{X}_1$ and $\vec{X}_2$, respectively.

It is shown in reference (8) that J is related to f by

$$J(\vec{x}, \vec{n}, E) = P^2 f(\vec{x}, \vec{n}, P)$$

where P is the momentum corresponding to the energy E. Putting this result together with equation (G6) into equation (G8) produces

$$J(\vec{x}_2, \vec{n}, E_2) dE_2 = J(\vec{x}_1, \vec{n}, E_1) dE_1 \qquad (G9)$$

Integrating equation (G9) produces equation (G4) which is the desired result.